CONTENTS

RECENT DEVELOPMENTS IN ATTEMPTS FOR CHEMICAL STORAGE OF SOLAR ENERGY

INTRODUCTION

It is not necessary for me to emphasize the importance of the subject of "Photochemical Conversion and Storage of Solar Energy". In essence all the attempts in this area can, in some way or other, be traced to attempts to mimic photosynthesis which has been nature's method of such a conversion. In Sir George Porter's words what is being attempted is to create an "artificial leaf" - a leaf which could perhaps surpass nature's gift to the animal kingdom in efficiency and turn over. What I propose to do is to present my appraisal of the Fifth International Symposium on this subject, held in Osaka from August 26 to August 31, 1984, which I was fortunate enough to attend through the kind assistance of the Tata Energy Research Institute. This appraisal will naturally be tainted by my own biases. While doing this, I will follow the divisions made by the Symposium Committee and present the various appraches being attempted.

The six plenary lectures were shared between four countries; two from Japan, two from USA and one each from Israel and West Germany. There were twelve invited lectures presented in two parallel sessions and the countrywise division was five from Japan, four from USA, one each from United Kingdom, Israel and France. In all 164 posters were presented; of them, one from India. Table I classifies the presentation in each area countrywise. India had actually submitted 11 posters but only one of them could be presented. There is a need for greater participation from India in this area of research, which may turn out to be quite important to our country blessed with abundant sunshine and a population expected to touch the one billion mark quite soon. We shall discuss the plenary and invited lectures while discussing the poster presentations under the different heads.

It was to be expected that Japan, the host country, would be a major participant in the conference. However, from the quality of the papers and the representation it was given at the plenary sessions and invited presentations, it was apparent that Japan has launched a major effort in the area of photochemical conversion and storage of solar energy. In fact, Japan seems to have established a lead in many areas of solar energy utilization. It was reported that Japan expects to meet 5% of its total power needs in 1995 by solar energy, including wind power. While it may not be relevant to the theme of this paper, it is pertinent to note that Japan has targetted the cost of single crystal silicon photovoltaic cells produced by Ribbon technology to be ~$ 4.00/W in 1985, ~$ 2.00/W in 1990 and $ 0.40 to $ 0.80/W in 2000. Amorphous silicon, right now being used only for watches, calculators, etc. is targetted for large size applications with 10% efficiency in not too distant a future. The substrate for amorphous silicon, which is now metal or glass, is attempted to be changed to ceramic or polyester. It is believed that in future, while central power stations may be based on single crystal silicon, private home power supply may be based on amorphous silicon. Japan's extensive effort in the area of chemical routes to trap solar energy stems from its assessment that this is a futuristic technology with viability being realised perhaps towards the end of this century.

Table I. Countrywise classification of presentations in the Fifth International on Photochemical Conversion and Storage of Solar Energy

Subject	Japan	USA	UK	Israel	Netherlands	W. Germany	France	China	Italy	Sweden	Switzerland	Australia	Yugoslavia	Brazil	Canada	Spain	Iraq	Portugal	Belgium	India (presented)	Total (presented)	India (not presented)
A. Photocelectro chemistry																						
1. Photoelectro-chemistry at semi-conductor surfaces																						
a) Plenary		2				1															3	
b) Invited	2	2		1																	5	
c) Poster	14½	7½	½	1	1		6½	3	1	2		1		1		1					40	2
2. Photogalvanic effect																						
c) Poster	1																1				2	6
3. Organic Photo-voltaic systems																						
c) Poster	6	1						2													9	
B. Photocatalysis																						
1. Heterogeneous																						
b) Invited	1						1														2	
c) Poster	20	2½				2	1	1⅓			$1\frac{5}{6}$	1½	⅓		½		1				32	2
2. Photoredoxreaction and Energy Transfer in Homogeneous Solutions																						
b) Invited	1		1																			
c) Poster	19½	$5\frac{5}{6}$	1⅓	3			1⅓	½	2		½	2			1				1	1	39	1
C. Biomimetism and Photosynthesis																						
1. Photoredoxreaction & Energy Transfer in Organized Molecular Systems																						
a) Plenary	1			1																	2	
b) Invited	1	1																			2	
c) Poster	13	3		2		1	2									1		1			23	
2. Mechanism & Simulation of Photosynthesis																						
b) Invited		1																			1	
c) Poster	4½	2				1	½														8	
D. Unimolecular Energy Storage Reactions & other topics																						
a) Plenary	1					1															1	
b) Poster	10					1															11	
	95½	$26\frac{5}{6}$	$2\frac{5}{6}$	8	1	6	12⅓	$6\frac{5}{6}$	3	2	2⅓	4½	⅓	1	1¼	2	2	1	1	1	182	11

The photovoltaic behaviour of a semiconductor - liquid electrolyte interface can be utilized either to effect photoelectrolysis, where light energy is converted to chemical energy in the form of the free energy of resultant products (fuels and hence storage) or to convert light energy into electrical energy through the use of what are called liquid junction photovoltaic cells or electrochemical photovoltaic cells. The incident light is absorbed in the semiconductor interface in contrast to photogalvanic cells where the light is absorbed by dye molecules in the electrolyte.

The two major problems of the photoelectrochemical approach to generate electricity or chemical fuels are (i) the corrosion that occurs when the semiconductor immersed in an electrolyte is subjected to illumination and (ii) the overvoltage. Both these aspects have been subjects of intense research and substantial success has been achieved in overcoming both these problems and the photoelectrochemical approach to trap solar energy appears to be a very promising route in the near future. The efficiency of liquid junction photovoltaic cells have been increased upto about 13% and stabilites close to that of amorphous silicon cells are reported. In fact the optimism runs so high that Adam Heller of Bell Labs has proposed that scientists should now start paying attention to the packaging problems of such devices. It is believed that future developments will depend on the detailed understanding of interface energies and kinetics for light-induced redox reactions at the semiconductor/liquid electrolyte interface. Also necessary to understand is the electric field distribution across the interface between the electrolyte and the morphologically and chemically complex semiconductor surface.

Roy Morrison (USA) has suggested that while surface films formed on the semiconductor surface, on account of either corrosion reactions or from side reactions leading to insoluble products (arising from poor selectvity in the photoelectrochemical process) or from ineffective cleaning of the electrode are usually deleterious; however, if the surface film is a semiconductor or insulator, a passivating film of 20 A° is often beneficial, since it leads to an efficient hole-electron separation. The problem however is to have a stable thin film of about 20 A° in photoelectrochemical cells. Current research on liquid junction photovoltaic cells is aimed at overcoming the corrosion problem, improve the efficiency and improve selectivity so that film formation and changes in electrolyte are avoided. Corrosion of semiconductor photoanodes can be reduced either by the presence of strongly reducing agents or by less reducing but highly concentrated redox systems.

A thin layer of conducting polymer films is also able to reduce corrosion and this method has been adopted with considerable success. Loading the conducting polymer with metal clusters (electron pools) enhances the efficiency in photoelectric synthesis of fuels such as hydrogen (Wrighton, USA and others). Wrighton has suggested the use of biological redox catalysts such as hydrogenases and nitrogenases instead of noble metals. The question to be answered pertains to the stability of the immobilized enzymes on the electrodes.

Adam Heller (Table II) has achieved an efficiency of 13.3% in photoelectrochemical production of hydrogen with p-InP photocathode which has a recombination passivated surface and sub-1000 A° dia. hydrogen saturated, rhodium islands. For high efficiency, it is necessary that the islands of electrocatalysts should be smaller than the exciting wave lengths of light allowing thereby the reduction and often complete elimination of light reflection and absorption losses, that are characteristic of metallic catalyst films. It is also required that the surface (i.e. lateral) diffusion length of photogenerated electrons must exceed the interisland distances. Thus, the density of the islands required is set by the quality of the semi-conductor crystal that controls bulk electron-hole recombination by the chemical passivation of recombination in surface states at "bare" interisland regions, and by the prevention of leakage through the barrier by chemical assurance of microscopic barrier uniformity. By simultaneously achieving all of these in p-InP, a lateral diffusion length

of 2μm has been reached leading to a 13.3% conversion efficiency.

The instability of narrow band semiconductors to oxidative photo-degradation and the poor catalytic properties of the semiconductor surface for many chemical reactions of importance are both alleviated by the promising strategy of modifying the semiconductor surface with an electrically conductive polymer incorporating catalytically active metal centres. The rationale of such an approach is that the combination of conductive polymer and catalyst provides a mechanism for the rapid removal and trapping of photo-generated charges from the semiconductor and for the catalysis of desirable redox reacttions. Such an approach has been extended by several workers to suspend photochemical diodes in aqueous solutions and this approach would be rightly described under photocatalysis.

Table II summarizes the posters presented in the area of photo-electrochemical syntheses of hydrogen and other value added products. Both CO_2 fixation and N_2 fixation are being vigorously attempted. Table III summarizes the various types of liquid junction photovoltaic cells being investigated with the overall object of increasing efficiency and decreasing corrosion. Here one should mention the research of Gary hodes (Israel) on Cd chalcogenide cells. He finds that with single crystal $CdSe_{0.6}Te_{0.35}$ with Cs-sulfide electrolyte, a solar to electrical conversion efficiency of 12.72% can be reached by optimising both the semiconductor surface preparation and the electrolyte composition. With $CuInSe_2/I_3^-$ (electrolyte) system, a conversion efficiency of 11.7% is reported. Addition of Cu^+ to the iodide electrolyte and the formation of non-native In_2O_3 layer on the surface leads to a very stable and efficient $CuInSe_2/I_3^-$ systems.

Although the band gap of $CuInSe_2$ (1.0 eV) is somewhat too small to ideally match the light distribution of the sun it still has properties which make it interesting as a material in solar cells. It has a sharp band endge due to a direct transition. The large absorption coefficient gives an absorption length of 100nm, which for moderately doped materials is in the vicinity of, or less than, the depth of the barrier region. The latter is advantageous if polycrystalline materials are used.

One of the major developments in the utilization of photoelectro-chemical cells is the adoption of thin films on substrates for electrochemical synthesis and photovoltaic cells. Many investigations to understand the effect of methods of preparations of the thin films, their subsequent treatments including doping, polymer coating, metal deposition etc. are in progress as seen in Tables II & III. Nakato and Tsubumora (Japan) have reported 8.2% solar to chemical conversion efficiency (AM 1) under no external bias for photoelectrolysis of hydrogen iodide into hydrogen and I_3^- with a photoelectro-chemical cell consisting of a Pt coated p-n junction Si photoanode, a counter Pt electrode and a cation exchange membrane. The p-n junction was formed by doping an n-Si single crystal wafer with boron at the surface. Alternatively a photocell with a Pt coated n-p junction Si photocathode, prepared by doping a p-Si wafer with phosphorus at the surface, also decomposed HI into H_2 and I_2 with 7.8% efficiency. For both types average thickness of the deposited Pt layer was 1 to 3 nm. For electrode stabilization heat treatment after Pt deposition was necessary. Tests for long stability showed that the photo current at the maximum power point fell to 75% after 4500 hrs. A new photovoltaic effect found in $Au/nTiO_2$ implying the increase of the height of the Schottky barrier at the $Au/nTiO_2$ contact, has been investigated carefully and it has been concluded that the effects arise from the mixed Schottky barriers of different heights due to the discontinuous contact of the metal layer. The SEM studies on Au layers on $Au/nTiO_2$ reveal cracks about 10 nm wide. It is also shown that high photovoltages can be generated under appropriate metal semiconductor contact.

Fujishma and Nakabayashi (Japan) have presented a new kinetic model for the interfacial charge transfer processes. The measured electron transfer rates in the "abnormal region" of high exothermicity are quite incompatible with the basic postulate of classical theories, namely that electron transfer rates are dependent solely on the solvent reorganisation energy which is represented by the dielectric properties of the solvent and the molecular volume of the reactants. The consideration of intramolecular vibrations of the reactants leads to modification of the line shape function of the density of states in the liquid phase and hence to an increase in feasibility of the direct hole transfer from the valence band of the semiconductor to the reducing agent.

Tomkiewicz (USA) has developed methods to characterise the electric field distribution across the interface between the electroyte and the semiconductor surfaces (perhaps modified chemically) in liquid junction solar devices. The techniques are based on electric field modulation of the system response followed by phase sensitive detection. The three techniques employed are Impedance spectroscopy, Electrolyte electroreflectance and Electric field-modulated photoluminescence. The system studied in detail was $CuInSe_2$ in either $S^{-2}/S/NaOH$ or $I^-/I_2/Cu^{+2}/In^{+3}$ electrolyte. From such studies it is possible to provide unique information on the effect of etching electrodes. It is hoped to answer whether the surface oxidation changed the charge accumulation modes at the interface while maintaining the space charge layer at the solid electrolyte interface as the sole driving force for the separation of light induced charge or whether the oxidation created a new distInct solid phase that can from a junction with the crystal in which the electrolyte does not play a key role.

Tributsch (West Germany) suggests that strong molecular interactions beween excited semiconductor interfaces and redox molecules could lead to kinetic and energy advantages. In such cases photogeneration of surface states, failure of the Schottky-model for the semiconductor electrolyte interface, restructurization of space charge layer and more step electron transfer reactions with surface bonded intermediate states may be involved. These concepts allow us to depart from most existing attempts to find classical semiconductor electrochemical systems where ideally energy bands and redox systems should exchange electrons by tunnelling in the presence of a minimum of interference of surface states. Such non-ideal systems are: (A) in photolectrolysis and photoelectrocatalysis e.g. RuS_2 where it has been shown that light induced chemical bond formation via d-states is crucial for oxygen evolution. It has also been shown that kinetical limitations encountered with oxygen evolving photoelectrodes like PtS_2 and RuS_2 could be overcome with semiconducting materials containing clustered transition metals in their crystal structure. This behaviour can be likened to the role of cluster centers in biological systems. RuS_2 electrodes are found to be corrosion resistant and have high quantum efficiency for photo-oxidation of H_2O to O_2 and Cl^- to Cl with visible and near infra-red light. (B) Ne materials for regenerative solar cells: FeS (pyrites with E_G = dia 0.95 eV) is a d-bon semiconductor that is able to undergo co ordination chemical surface reaction an works as an electrode in solar cell producin electricity. I^-/I_3 stabilization is possibl however, the efficiency (1%) is very lo now and improvement should be attempte by controlling and modifying surface state which arise from transition metal complexe formed due to strong photoelectrochemic interactions. (C) Photointercalation Sola Cells and optical information storage: Stron molecular intercalation also occurs betwee intercalating semiconducting host materia (e.g. Cu_3PS_4, Cu_6PS_5I) and guest ior (e.g Cu^+, Ag^+) when excitation of electro into the conduction band makes intercalatic possible. Photointercalation has many possib applications such as photointercalatic batteries, photon powered ion pumps, info mation storage and photocatalysis (Zeolitie MoS_2, RuS_2 etc) Neither existing electr transfer models or conventional semiconduct liquid junctions modes are adequate in descr bing these photoelectrochemical mechanism involving strong electrochemical interaction

Fujishima, Honda and others (Japa have utilized the strong ability of phot excited surfaces to react with various kin of materials for image formation and phot floation. TiO_2 film about 1 μm on sheet formed by heat treatment of Ti pla has a hydrophilic character. A monolay coating of stearic acid, paraffin etc. chang the character to be hydrophobic. A fe seconds of irradiation of the coated surfa reverses the character to be hydrophil and hence such coated TiO_2 surfaces a useful for printing. Again coated TiC powders would float on water because hydrophobic character. Illumination sen the more efficient (in a photosense) particl to the bottom and hence this process c be used to select photoefficient particl

Organic photovoltaic solar cells ha received growing attention because of th potential low cost, simplicity of devi fabrication and the variety of compour available with absorption matching t solar spectrum. Generally energy conversi efficiencies reported todate for orgar solar cells are very low, though sunlig efficiences of about 1% have been report

for merocyanic dyes. Lower conversion efficiencies of organic solar cells relative to inorganic cells have been attributed to relatively low photocarrier generation efficiency, low mobility of charge carries and high electrical resistivity in organic compounds. The bulk resistivity could be decreased by doping. Table IV is a summary of the posters presented on organic photovoltaic cells including one on the concept of a plastic photo battery based on the idea of reversible doping of a polyacetylene film.

The research effort on photogalvanic cells in which the photon absorption by the liquid electrolyte leads to electrochemical changes, has taken a precIptious drop because of the realisation that such cells, though extremely simple to be fabricated and studies in detail, do not appear to be viable as practical solar electrochemical cells because of extremely low efficiency. Among the eight posters slated to be presented in this area none of the six abstracts submitted from India were presented at the conference. Most of such studies in India have been focussed on dyes which could be coated on the electrodes and could hence lead to realisation of organic photovoltaic cells.

Table II. **Summary of posters on photoelectrosynthesis**

	Electrode/Electrolyte	Reactants	Products	Remarks
1.	Fe (II) Tetraphenyl porphyrin-coated p-type GaP electrodes in 0.5 M H_2SO_4 (Yoneyama et al. Japan)	CO	Methanol (main) + some methane	-
2.	nCdS in halide ion containing aqueous solution stabilized by the use of a polymer coating-pendant Ru $(bipy)^{2+}_3$ moieties (Rajeshwar, USA and Kaneko et al, Japan)	Cl^-, Br^-	Cl_2, Br_2	quite rugged
3.	Polythiophene on gold electrodes with inclusions of Ag° & Pt° aggregates (Garner & Tourillon, France)	H^+ (pH=0)	H_2	Seems stable for 170 hrs.
4.	Amorphous-Si electrode (either p-i-n or p-i-n-p-i-n) on glass or stainless steel with Pt	H^+	H_2	Unstable; treatment increases stability

TABLE - II

	Electrode/Electrolyte	Reactants	Products	Remarks
	film on surface (15A°) (Matsumara et al. Japan)			
5.	n or p-type semiconductor electrodes (Fe, C, In or illuminated single crystal p-GaP cathodes) and stainless steel or illuminated polycrystal-line n-TiO_2 as anode) (Monheit et al, Israel)	a) 1 MNa_2CO_3 (with TiO_2) air-bubbled b) 6 MKOH with N_2 bubbled (with p-GaP)	a) NH_3, Formal dehyde & methanol b) ammonia	Also studied N_2 fixation with aqueous suspensions of TiO_2
6.	p-GaP coated with thin layers of Au, Zn or Pb (either by sputtering or electroplating) as photo-cathodes in 0.1M aqueous solutions of $(C_2H_5)_4$ $NClO_4$ or $(C_2H_5)_4$ NBr or $(n\text{-}C_4H_9)_4$ NBr (Ikeda et al, Japan)	CO_2 bubbled	CO + Formic acid and H_2 from water No alcohol, aldehydes and other carboxylic acids	
7.	SnO_2/Si photoanodes with thin Pt film (Schimizu et al, Japan)	Water	Electrolysis	Photo-assisted electrolysis
8.	Single crystals & poly-crystalline n-TiO_2 coated with Au or Pt by sputtering electroplating or photo-chemical deposition (Chin-hua et al, China)	Water	Electrolysis	Role of metal catalyst studied
9.	p-InP (Nozik et al, USA)	Water	H_2	Theoretical studies on effect of hot electron injection
10.	Recombination-passivated surfaces of p-InP photocathodes having < 1000A° diameter, hydrogen- saturated Rh islands (Heller, USA)	Water	H_2	13.72% efficiency for chemical storage in the form of hydrogen ; investigated the effect of size of islands.

Table III. Summary of posters on semiconductor-electrolyte junction photovoltaic cells

	Electrode/Electrolyte	Characteristics	Remarks
1.	n-SnO_2/p-Si in acidic solution (HI) (Nogami, Japan)	Both photoanodic and photocathodic effect. Maximum photocurrents under cathodic and anodic biases were 5-10 mA/cm^2 in acidic solution with illumination of 60 mw/cm^2	Oxygen-reactive Sputtering of Sn on to a single crystal of p-Si ; SnO_2 film $\sim$800-1000A°, Aim is to prepare a metallized (Pd or Ru) heterogeneous photocatalyst with alternative reduction and oxication achieved.
2.	n-type porous Si (N_2 bubbled when used as photoanode) with Pt as counter electrode (Koshida et al, Japan)	Saturation photocurrent proportional to illumina tion (O_2 & H_2 evolved at the n-Si and Pt electrodes)	Thick anode film; anodization carried out under illumination; Porous structure stabilizes photoanodic operation.
3.	SnO_2 thin films ($\sim$500A°) on indium-tin oxide substrates with Sb or F as dopant ; 0.1 M $NaClO_4$ in acetoitrile as electrolyte. Photo sensitizers ; Rhodamine B and Rose Bengal ; Hydroquinone as supersensitizer (Itoh et al, Japan).	Highest level of quantum efficiency obtained with donor density $=\sim 4 \times 10^{20}$ cm^{-3} and Hydroquinone = 0.01 M; was 0.33 for Rhodamine B and 0.87 for Rose Bengal	Prepared by vacuum deposition and spray pyrolysis. Photocurrent quantum efficiency depends on donor density.
4.	Noble metals supported on TiO_2 (photo deposited) or electrodeposited or chemically adsorbed on	70% enhancement in photocurrent after 8 hours of photodepositing Au on TiO_2 surface	Improvement possible due to faster chemical kinetics, a more favourable electron transfer

TABLE - III

	Electrode/Electrolyte	Characteristics	Remarks
	the surface of reduced ceramic TiO_2 electrodes) (Pollock et al, USA)	(almost maximum attainable)	mechanism and improved modification in the surface states (no change in band gap). Catalytic islands of Au metal for optimal geometric configuration should be smaller than the wave-length of the radiation and closer together than the depletion width.
5.	TiO_2 and Pt–TiO_2 in 1 N H_2SO_4 (Chongyang et al, China).		Elementary steps in electron transition through surface states on photoelectrode, directly defined.
6.	TiO_2 (Rutile) single crystal slice (cut perpendicular to C-axis) electrode platinized by electrochemical or photocatalytic deposition in 0.5 M H_2SO_4 (Uosaki et al, Japan)		C - V relations show that platinization reduces the over potential of hydrogen evolution reaction. Mott-Schottky plots show that the effect of platinization on space charge capacitance is small. Results suggest that Pt is a catalyst for hydrogen evolution but has no role for oxygen evolution in photolytic decomposition of water.

TABLE - III

	Electrode/Electrolyte	Characteristics	Remarks
7.	TiO_2 film (anatase) prepared by Sol-Gel method on nesa glass (photocathode) with Pt as anode (Yoko et al, Japan)	Maximum photocurrent ~13 mA cm^{-2} at 1.5V	Photocurrents depend on thickness with maximum around 1.5-1.8 μm ; vigorous gas evolution seen on illumination at both electrodes.
8.	TiO_2/aqueous solution interface (Aikawa et al, Japan)		Photogenerated surface states have been characterised.
9.	$SrTiO_3$ doped with La^{3+} (Chang, Japan and Clavrie and Campet, France)	Photo response similar to that of mechanically polished samples	Photoresponse in visible region is attributed to structural defects caused by doping element besides impurity states located within the band gap.
10.	n-Si/Th(III) oxide heterojunction - Thin film photo-electrochemically deposited on a single crystal. n-Si - photoanode with Pt as cathode ; alkaline solution of ferrocyanide/ ferricyanide (Switzer, USA)	V_{OC} = 0.5112V J_{SC} = 33.5 mA/cm^2 Fill factor = 0.680. 14.6% photovoltaic efficiency (with IR filtered xenon light at 80.0 mW/cm^2) 11.0% with 75.3 mW/ cm^2 natural sunlight and 22.3% with 800 mm (η = 97%)	n-Si wafers of (100) orientation gave higher photovoltages than (111) wafers.
11.	Single crystal Cu_2O (p-type) with Pt counter electrode in 0.1 N NaOH and 0.1 M $CuSO_4$ solutions	Illuminated with a 500 W Xe lamp - Not very good photo response and poor stability	

TABLE - III

Electrode/Electrolyte	Characteristics	Remarks
(Takeuchi et al, Japan and Weichman, Canada)		
12. αFe_2O_3 - defect doped or substitutionally doped (Houlihan et al, USA)	a) Defect doped either by heating to high temperature and then rapidly quenchng or by subjecting to various reducing atmospheres at high temperatures	Mossbauer effect ESR etc. used for characterisation. Photocurent studies as a function of annealing, temperature etc.
	b) Substitutional or Stoichiometric doping with Si^{4+}, Zr^{4+}, Ru^{3+}, Nb^{5+}, Ca^{2+}, Cu^{2+}, Mg^{2+}	Deposition of Ru on defect doped Fe_2O_3showed increase of photocurrent.
13. $CuInSe_2$ (Band gap 1.0 eV)-Polycrystalline thin film $CuInSe_2$ (0.7-2μm thick) electrodes prepared by codeposition of elements Cu, In and Se in vacuum (on Alumina substrates furnished with a thin layer of Mo)-(Lindgren and Lindquist, Sweden)	Photovoltage of 50-150 mV with polysulfide system and I_3^-/I^- system. Etching in 1 MHC1 for 3 min leads to increase in both V_{oc} and I_{sc} as well as the improved dark current characteristics. These effects improve further with a subsequent Zn^{2+} solution treatment. For best preparation I_{sc} = 10 mAcm^{-2} for 100 mWm^{-2} (white light).	It is possible to vary the stoichiometry of the layer with the distance from the rear contact.

TABLE - III

Electrode/Electrolyte	Characteristics	Remarks
14. nGaAs - photoanodes with NaI solution (Allongue et al, France).	In netural 7 M NaI solution passivating phenomenon observed. In acidic medium (HI or H_2SO_4) with $[H^+]=5x10^{-3}$ M, passivating phenomenon disappears and stabilization of photocurrent after 6 hrs. seen. $V_{oc}=450mV$ with $10^{-3}M$ Iodine concentration. Band edges positively shifted by 0.18 and $V_{fb}=0.82$ V vs SCE.	To verify if very concentrated electrolytes are able to stabilize nGaAs owing to (i) the negative shift of V_{redox} with iodide concentration increase and (ii) the high solubility of iodine in such solutions.
15. Single crystal n-Ga(As,P) alloys made by epitaxial growth on a binary single crystal substrate with metal organic vapour phase epitaxy technique. Type A is with GaAs single crystal substrate and Type B is with GaP as substrate. (Carlsson et al, Sweden)	Rotating Disk with semiconductor disks-studies made. In the series $GaAs_{1-y}P_y$ cross-over between indirect (as in GaAs) transition occurs at y=0.45. For y=0.55 band gap is 2.00 eV (λ 620 nm and the lower boundary of the direct transition is 2.15 eV. Type B is found to show good photoresponse.	To demonstrate how the properties depend upon material preparation, composition determined by the SEM microprobe technique.
16. n-GaAs stabilized by polythiophene ; protected n-GaAs electrodes in ferro-ferricyanide aqueous solution. (Horowitz and Garnier France)	In polypyrrole stabilized n-GaAs, film peeling occurs in 10-20 minutes of operation. With poly (3-methyl) (thiophene films, long term stabilization (~100 hours). seen. Efficiency measured with a source	Deposition of a protective thin layer stabilizes small band gap semiconductors - conducting poly 3 methyl thiophene used. Pre-deposition of 2 nm thin film of Pt was necessary.

TABLE - III

Electrode/Electrolyte	Characteristics	Remarks
	and long pass (515 nM) filter is 11% with illumination of 14 mW/cm^2	
17. n-type III-V semiconductor electrode in aqueous electrolytes eg n-GaAs $1M(Se^{2-}/Se^{2-}_3)$ + 1M KOH; n-GaAs in 1M KOH and 8M $NaClO_4$ (Allongue, France).	Rate constnts that describe photoconversion and oxidation of Se^{2-} obtained ; and Ru treatment improves stabilization and performance of n-GaAs/Se^{2-} cells because of the catalytic effect of Ru on the hole transfer towards solution. In highly concentrated electrolytes corrosion rate constant is lowered while the H_2O activity is reduced confirming that water molecules are reactant in the photocorrosion process of III-V semiconductors.	Kinetic stabilization of n-type III-V semiconductor elecrodes investigated.
18. Thin films of Zrs, prepared by gaseous sulfidation of Zr sheet stabilized by alkaline polysulfide solution. (Bradhurst and Tuffy, Australia)	Photocurrent density = 0.25 MA/cm^2 in AM_o sunlight and a flat band potential of -0.7V (SCE).	

TABLE - III

Electrode/Electrolyte	Characteristics	Remarks
19. Ru electrodeposited on Cds (polycrystalline thin films) (Jimenz et al, Spain)	A very small stabilizing effect (~20 mins) at low illumination intensity noted with 2 monolayers of Ru deposited. This stabilizing effect decreases considerably with increasing illumination intensity.	Stabilization of CdS against photoconversion by electrodeposition of RuO_2 on thin films attempted.
20. Thin film CdSe electrode prepared by electrodeposition of Ti substrate; Electrode annealed at 550°C for 30 min in air. (Wang et al, China)	a) $Fe(CN)_6^{3-}$/ $Fe(CN)_6^{4-}$ (alkaline) with Pt as counter electrode-9.6% energy conversion efficiency with 500 W Tungsten-Bromide lamp, b) Na_2S, S, OH^- - 3.5% energy conversion efficiency. c) Etching of anode effected with different solutions- Best (12.1%) efficiency obtained with etching for 20 secs with 3% Br_2/CH_3OH followed by etching for 15 secs in a mixture of HNO_3:HCL: H_2O = 0.5:4.5:5 for 15 sec. d) Dipping anode in H_2PtCl_6 solution for 30 secs after 20 secs etching with HNO_3:HCl:H_2O = 0.3:9.7;90 gives energy conversion of 12.1% and good stability for at least 32 hrs. Addition of Se to electrolyte also increases stability.	

TABLE - III

	Electrode/Electrolyte	Characteristics	Remarks
21.	Electrophoretically deposited CdSe on SnO_2 coated glass anode polysulfide electrolyte/Pt (Minoura et al, Japan)	a) Photoanodic dissolution in an aqueous solution (photoetching) or b) soaking of the CdSe electrode in Zn^{2+} ion containing electrolyte ; SEM studies made. Results indicate that the Se at CdSe surface interacts with polysulfide ions, forming new surface species with energy levels within the forbidden gap. These surface states may contribute to the enhancement of the reversibility of the sulfide/polysulfide reaction.	Effect of surface-treatments of CdSe - Both (a) or (b) lead to increase in V_{SC} and I_{SC}. Best results obtained : 7% energy conversion efficiency (white light).
22.	n-CdTe films electrodeposited with a pulse current on Ni substrate from a solution of 0.5 m $CdSO_4$, TeO_2-saturated, 10^{-2}% $In_2(SO_4)_3$ at pH=2 to 3. (Xunnan et al, China)	With 50 mW/cm^2 irradiation n-CdTe/1M Na_2S; 1 MS, 1 M NaOH/C cell has 3% energy conversion efficiency with V_{OC} = 0.5 V & I_{SC} = 7.6 ma/cm^2. A lead acetate solution etching of CdTe anode improves efficiency and stability.	Effects of deposition conditions studied.
23.	CdSe/CdS/Al thin films on Al substrate in aqueous ethanol solution. (Fujii, Japan)	Double layer electrodes of CdS/CdSe shown to have better photoefficiency than single layer CdS/CdSe electrodes.	The heterojunction CdS/CdSe double layer increases the effectiveness of charge separation.

Table IV - Organic Photovoltaic Systems

	Electrode/Electrolyte	Characteristics	Remarks
1.	Au/Phthalocyaninato Zinc (II) (p-type) (~50 mm thick)/ 5, 10, 15, 20-tetra (3-pyridyl) porphyrin (TPyP) (n type) (~40 nm thick)/Al (Yamashita et al, Japan)	Quantum efficiency of photocurrent for thinner TPyP film (~7 nm) is found to be 17%. A phenomenon of co-sensitization found with thin films. V_{OC}~1V ; Maximum power conversion efficiency with 10 $\mu W/cm^2$ at 430 nm reaches 2%.	It is shown that the photoactive region is the ZnPc/TPyP interface. The p-n junction cell comprising ZnPc and TPyP is among the most efficient organic PV cells known so far.
2.	Electropolymerization of a variety of metallo-protoporphyrins free acids to produce excellent quality films on NESA glass, Ag Pt and some semiconductors (Ginley and Shelnut, USA)	High quality films obtained with Cu-, Ni-, and Zn - but not Fe (III)- and Sn (IV) - Protoporphyrins - presence of axial ligands affect ability of monomer to polymerize. Oxidative polymerization of vinyl groups has been possible on a number of the metalloporophyrins.	Resonance Raman studies made. Absorption spectral changes due to (1) saturation of the vinyls, (2) excition coupling and (3) aggregation of the porphyrin rings in the film. Studies on immobilization of metalloporphyrins on an electrode surface.
3.	X-form metal free phatalocyanine ($X-H_2Pc$) thin films on Indium Tin oxide, Al, Pb or CdS were used as barrier	With $Al/X-H_2Pc$-polymer/ ITO polyvinylidene fluoride used as a binder gave larger I_{sc} but smaller V_{oc} and fill factors than with polyvinylacetate as binder.	Studied the effect of binder polymers.

TABLE - IV

	Electrode/Electrolyte	Characteristics	Remarks
	electrode materials. (Minami et al, Japan).	Pb was better than Al but CdS gave the most encouraging performance.	
4.	Coumarin-6 vacuum deposited on base electrodes such as SnO_2, In_2O_3, Pt, Au & Pd (surface concentration at about 25 n mol cm^{-2}); pH varied from 0.4-7.0 (buffer solutions) - acted as a photocathode independent of base materials (Mizutani et al, Japan).	Quantum efficiency changed from 1.5 at pH 5 to 7 to about 7% at pH below 3.5	The increase in efficiency at lower pH is attributed to the protonated species being formed.
5.	Polyacetylne film formed by electrochemical technique (Huang et al, China).	Polymerization process can be controlled by the wave form of electric current and the composition of the solution.	A method for preparation of controlled polyacetylene film on electrodes, such as Ni, Cu etc.
6.	Photodoping of polyacetylene thin film for possible photoenergy storage (Aizawa et al, Japan).	Electrochemical oxidation or reduction of polymer matrix initiates anion or cation doping. Doped electrolyte is undoped in a discharging process. Studies made on photoelectrochemical doping instead of just electrochemical doping.	Concept of a plastic photobattery
7.	Quinacridone dyes dispersed in polymer binder and applied as thin film on In_2O_3 coated	Using 2, 9 dimetnyl quinacridone as pigment : $J_{sc}=1.58 \mu A.cm^{-2}$.	Several quinacridine pigments studied. Good : unsubstituted

TABLE - IV

	Electrode/Electrolyte	Characteristics	Remarks
	thin film on In_2O_3 coated glass electrode. Al electrode was evaporated on film to form a sandwich type cell (Yokoyama et al, Japan).	(500 nm ; 2.7 m W/cm^{-2}) V_{oc}=1.15 V Fill factor =0.25 to 0.3 Conversion efficiency = 0.34% $J_{sc}=I^n$ with n=0.6 to 0.7 for intensity of the order of 0.1 mW/cm^{-2} at 550 nm.	2, 9 dimethyl; 3, 10 dimethyl quinacridones. Poor: 4, 11 dimethyl; 2, 9 dichloro; 3, 10 dichloro quinacridones
8.	Electrochemically doped poly (N-vinyl carbazole) (PVCz). In/PVCz/Au cell (Shirota et al, Japan).	Thin films of PVC cast on Pt electrochemically doped by controlled potential anodic oxidation at 1.0 V vs Ag/Ag^+ 0.01 mol cm^{-3} reference electrode in the presence of tetra-n-butyl ammonium perchlorate in acetonitrile. The thin film after drying is peeled off and used as sandwich between semi-transparent Au and In metals (Vacuum deposited on each side of the film). Power conversion efficiency ~1.1 X 10^{-2}%	

The strategy to use a photosensitizer, which would absorb the solar radiation to reach its excited state, whose redox potentials are more favourable for electron transfer reactions (either reduction or oxidation) than the ground state, has been the subject of intense investigation for several years. In principle the following are the usual sequence of reactions of water photolysis

$S \xrightarrow{hv} S^*$ S- sensitizer

$S^* + R \longrightarrow S^+ + R^-$ R - usually termed relay

$S^+ + D \longrightarrow S + D^+$ D- donor is also a relay

$D^+ + H_2O \xrightarrow{catalyst} O_2$ - oxidation

$R^- + H_2O \xrightarrow{catalyst} H_2$ - reduction
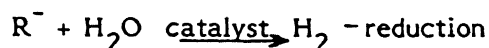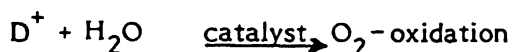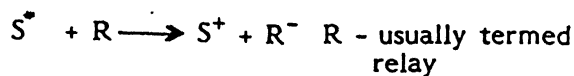
Several modifications of this sequence exists and the system may be homogenous or heterogeneous. In all cases the associated problems are the efficient coupling of oxidative and reductive parts and separation of the evolution of H_2 and O_2 in the case of water photolysis. The life times of S^*, the quantum efficiency of formation of S^*, the rates of electron transfer and the rates of recombination of charged species, the turn over number of the catalyst are the important parameters that control the efficiency of the system. Also important is the spectral response of S which has to be tuned to achieve maximum absorpotion of the solar spectrum. At this conference it was generally agreed that the homogenous catalysis route is not viable especially because of its inherent inability to retard back electron transfer reactions leading to recombination of charged species. However, it was emphasized several times that much of our understanding of heterogeneous systems stems from the investigations carried out on homogeneous systems which are free from the usually ill-understood surface effects.

In the area of homogeneous catalysis, the main target is to identify new sensitizers and as yet no better candidate than Ruthenium $(bipyridyl)_3^{2+}$ has been realised. $Ru(bipy)_3^{2+}$ - excited state energy, 2.12 eV, is too high and results in the fraction of solar energy trapped being very poor; life time of single state 0.6 μs is reasonable and so is the oxidation potential of the excited state (E_{ox}=-0.87V). The tuning of the excited state energy by substitutions in the bipyridyl moiety has been attempted for several years.

From Table V which summarizes the posters presented on homogenous systems, it is apparent that while a variety of sensitizers (Prussian Blue, Eosin Y, Rose Bengal, Fluorescein etc)are being studied, one is far from a satisfactory candidate. One of the possibilities is to use a triplet excited state. The other questions to be answered are: (a) what is the importance of polarity of the volvent? (b) can we have some standard conditions (may be even a standard catalyst) for comparing and standardising quantum yields, turn over numbers etc.

The other important subject of study is the design of the relay, the most popular one being methyl viologen. The coupling of relays to donors and acceptors to hasten charge separation and avoid back transfer has been attempted (see Table V). Here again the stability of the relay is an essential requisite. Even Fe^{2+}, Hg^{2+} are being considered for the role of acceptors.

Table VI, which outlines the posters presented in the area of heterogenous photocatalysis, reveals the collosal effort that this area has attracted. It is a relatively new exciting field and poses challenge to our ability to design materials based on bulk solid state and surface characteristics. This area has benefited from the outstanding achievements in the area of semiconductors. In fact much of the promising work has emanated from laboratories which have a rich tradition in the area of material sciences. The catalysts studied are varied; the surface treatments, metallization etc. are extremely innovative. Some of the important presentations are outlined below.

Tazuke (Japan) discussed the problem of of back electron transfer in electron transfer sensitization especially in homogeneous solutions. An excited state can be quenched by a

quencher via electron transfer process. Processes occuring are essentially those encountered in any typical exciplex formation kinetics. The ion-pair formed yields cation-anion pair. The recombination of these ions should be prevented and maximum charge separation should be achieved. Many groups have used the following strategies for this :

1) Charge separation by Coulombic separation,
2) Use of colloids, micelles, polymers, etc.
3) Use of destructive oxidant/reductant.

Examples for Coulombic separation are :

1) (RuL_3^{2+}) can be quenched by an oxidant or reductant. When the substrate is oxidant charge separation will be inefficient. When the substrate is reductant charge separation is efficient. In the former case ΔS controls the processes. In the latter the efficiencies correlate with ΔH. These are to be borne in mind and Marcus theory must be applied.
2) Benzophenone interacts slightly with leuco-crystal violet. But benzophenone substituted with $-NR_3$ interacts far better. This is due to Coulombic effect. Similar effect is noted by addition of salts. All these effects are understood in terms of ionic strength. In many cases log k_q(k_q is quenching constant) gives linear plots with $\mu^{1/2}(1+\mu^{1/2})^{-1}$

It is interesting that the Debye-Huckel theory and the well-known concepts in chemical kinetics regarding salt effects can be applied to excited state reactions. Whenever the excited species and quencher are both charged k_q increases with μ. Tazuke discussed two other systems also. In most of the systems chosen by him, the two entities, viz. excited state and the quencher were both charged species. Hydrocarbons used in one case were attached to water soluble materials to which an anionic or cationic group was fixed.

Harrman (U.K.) considered a few sources of hydrogen other than water and proposed a design for photosystems capable of producing H_2 from such substrates under "homogeneous" conditions using metalloporphyrins as the photosensitizers. The substrates suggested are H_2S, S, hydrazine, alcohols, carboxylic acids and sugars. A suitable metalloporphyrin plus colloidal Pt could be an effective photocatalyst. In case of H_2S, sulphur poisoning of the catalyst inhibits the reaction. Tin (IV) porphyrins are good photosensitizers for alcohol and related substances and high yields of H_2 are indeed realised.

Among heterogeneous systems the major effort has been on effecting surface modification of the semiconductor catalysts by platinization, dye-coating etc. Frank (USA) and Honda (Japan) presented data on surface-modified single crystal CdS photochemical diodes suspended in aqueous solutions. The surface modification involved coating the faces of CdS with electrically conducting polypyrrole and catalytic dispersions of transition metals (Pt, Rh, RuO_2) immobilized in polystyrene film. The combination of polypyrrole and catalytic polystyrene films prevented photo-induced dissolution of CdS and catalysed H_2 and O_2 evolution. The amount and composition of metal dispersed in the polystyrene-coating affected charge transport and electroactivity of the semiconductor. These factors and the hydrophobic nature of the polystyrene films were important in achieving good catalytic activity and stability of the CdS semiconductor. Sorption processes and the electronic contact between the polymer and the semiconductor also influenced the net yield of H_2. (Polypyrrole fixed the catalyst to surface). Rhodium black was the most effective catalyst for hydrogen; the overpotential is less than for Pt black. A new method for oxidative deposition of Pt is by decomposition of $[Pt_3(CO)_6]_4^{2-}$ - [JACS, 96, 2614 (1974]. Pt clusters (.5%) produced on TiO_2 this way are 10 times more effective than .5% Pt on TiO_2 deposited other ways. This effect must be due to the size of the clusters.

Amouyal and Koffi (France) have characterized the system $Ru(bipy)_3^{2+}/MV^{2+}$/EDTA/colloidal Pt by measuring hydrogen quantum yields as a function of the concentration of the different components in the system. Compared to a theoretical limit of 18%; quantum yield of 17% has been obtained at pH $\sim$ 5, $Ru(bipy)_3^{2+}$ = 5.6×10^{-5} M; EDTA = 0.1 M; Pt = 0.5%. Quantum yield increases with MV^{2+} and reaches a plateau. Under optimal conditions, various types of heterogeneous catalysts (colloidal metals, metal deposited on semiconductor powders, metal and metal oxide powers) have been tested and compared. Radiolytically prepared colloidal metals seem to be better because of smaller sizes and uniform distribution of size. Among the noble metals, Ir is the best : Ir $>$ Pt $>$ Os $>$ Ru $>$ Rh; Cu, Co & Ni and metallic oxides have also been tested. Pt black is not as efficient as colloidal Pt.

For chemically prepared colloids, particle size of Pt or Ir does not seem to matter, except when the size is too small and the yield drops down drastically. Pt deposited on TiO_2 is not as effective as colloidal Pt.

In the panel discussion Shilov (USSR) emphasized the role of poly-nuclear clusters; very little study has been made on the possible role of cluster compounds.

Considerable enthusiasm was generated by the report of Sakata (Japan) and others on application of photocatalytic reactions using semiconductors and dyes for organic syntheses. The photo-Kolbe reaction of converting carboxylic acids to hydrocarbons (originally reported by Bard) was studied with Pt/TiO_2 and shown to have side reactions, one of them being

$$CH_3COOH + 2H_2O \longrightarrow 2CO_2 + 4H_2$$
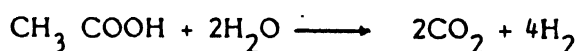
Hydrogen production has also been obtained from C, alcohols, sugars, cellulose, hydrocarbons and fatty oils. There appears to be selectively depending on the catalyst used. For example,
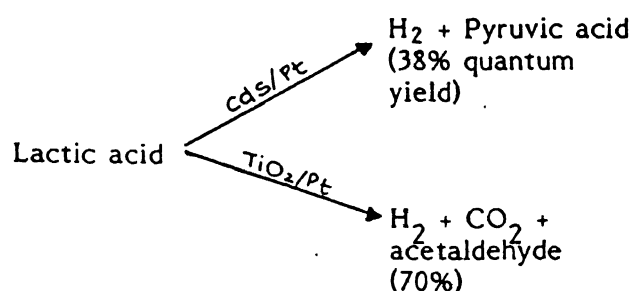
Photocorrosion of CdS was found to be suppressed during the reaction and the photocatalytic activity was maintained for more than 300 hours irradiation. Also
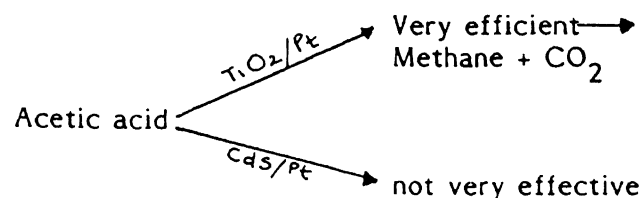
Aminoacid production by irradiating a mixture of various organic compounds and ammonia with UV light has been investigated mainly from the view point of chemical evolution. Bard and Reiche had demonstrated the formation of various amino acids from CH_4-NH_3-water with Pt/TiO_2. Kawai has reported the formation of polypeptide and amino acids with glucose-ammonia-water but with low yields. By use of semiconductors and dyes, high efficiency has been achieved (quantum yield 20 to 40% with visible light) without metal catalysts such as Pt. The reactions are selective and depend on the kind of semiconductor and can be classified into 3 types :

(1) Keto carboxylic acid, NH_3, triethanolamine (sacrificial) e.g. 2-ketoglutaric acid $+ NH_3 + 2H^+ \xrightarrow{2h\nu}$ glutamicacid 30% quantum yield with ZnTPPS as catalyst (436 nm) Pyruvic acid $\xrightarrow{2h\nu}$ alanine

(2) Hydroxycarboxylic acid (no sacrificial agent needed since the acid acts as the reducing agent), NH_3
Lactic acid $+ NH_3 \xrightarrow{2h\nu}$ alanine
18% quantum yield with CdS (430 nm)

(3) Unsaturated carboxylic acid, NH_3 (addition of NH_3)
acrylic acid $+ NH_3 \xrightarrow{h\nu}$ β-alanine
42% yield with acridine yellow (450 nm)
38% yield with Zn TPPS (436 nm)

By introduction of an assymetric catalyst one can even achieve asymmetric synthesis.

Hybrid catalysts, in which either hole-electron separation is increased or CB/VB levels are increased, are expected to play a key role in selective synthesis of organic compounds. Fixing dyes or enzymes on such hybrid catalysts could improve the efficiency. It is expected that research on photocatalysts would have many sided applications besides production of hydrogen from water and conversion of solar energy into electricity and have bearing on many problems :

(a) Production of energy rich materials, selective transformation of organic molecules
(b) Fermentation processes
(c) Origin of life
(d) Fuel cell technology
(e) Environmental studies (pollution and disposal of wastes)
(f) Semiconductor processing
(g) Information storage

What is likely is that research will shape along the following lines :

(a) Search for new semiconductor materials

(b) Preparation of hybrid catalysts and their modification

(c) Surface design of semiconductors by implanting materials at micro depth levels

(d) Combining materials for mimicking functions

In this conference there was little added by way of improving the existing theories on the maximum attainable solar energy efficiencies. Willig and co-workers (W. Germany) pointed out in a poster that the high efficiency predicted for solar energy conversion (e.g. loss) does not take into account any of the details of the subsequent process of charge separation; taking into account the charge separation leads to a decrease in efficiency by about a factor of three for the reaction centre. The main cause for this significant free energy loss in this real molecular device appears to arise from reorganisation effects. The question is whether one can build an artificial molecular device that is closer to the upper efficiency limit than the primary process in bacterial photosynthesis. It is expected that in solids, such as in certain organic single crystals where charge transfer occurs between isoenergetic levels with a hopping time of the order of a few picoseconds at room temperature, reorganisation effects play a much smaller role than in electron transfer reactions in polar solvents. Hence solid state molecular model systems are being investigated.

In a similar vein, Moggi and Balzani (Italy) have modified the equations, which relate the chemical potential of the excited state to the efficiency of conversion in the case of an ideal photosensitizer (perfect absorber and emitter) to account for extinction coefficients and life times of real photosensitizers. It is found that the efficiency depends on the ratio CV/A where C is the concentration of the ground state photosensitizer, V the reaction volume and A the irradiated area. It is also shown that the best conditions for solar energy conversion are when

$$\Delta\mu_r^{\circ} = \Delta\mu_s^{opt} \quad \text{where} \quad \Delta\mu_r^{\circ} = \mu_P^{\circ} - \mu_R^{\circ}$$

for the reaction

$$\text{R (Reactants)} \xrightarrow[S]{\text{sunlight}} \text{P (Products)}$$
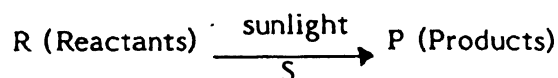
and $\Delta\mu_s^{opt}$ = the difference between the chemical potentials of the excited and ground states of the photosensitizer.

A solar-pumped Nd - YAG laser, where a solar energy collector consisting of a paraboloidal mirror 10 m in aperture and 3.2 m in focal length is used to pump a water-cooled Nd - YAG laser rod 4 mm in diameter and 75 mm in length, has been successfully developed (Arashi et al, Japan-Japanese J. App. Phys. 23, 1051 (1984). The maximum output of the laser is 18 W in multimode, and is the highest output power reported so far in solar pumped laders.

Table V : Summary of posters presented on Homogeneous Photocatalytic Reactions
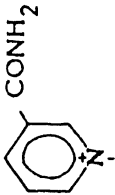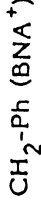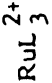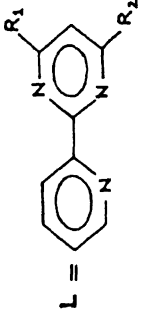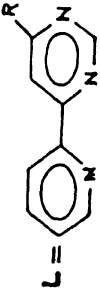
	Sensitizer	Relay	Redox System	Remarks
1.	$Ru(bipy)_3^{2+}$ (Wada et al, Japan) [structure: pyridinium ring with $CONH_2$, N^+] CH_2-Ph (BNA^+)	Aliphatic amines (aromatic amines do not act as as relays)	(BNA^+) in methanol (A model for NAD^+) $BNA^+ \xrightarrow{h\nu} BNAH + BNA_2$	NAD^+/NADH & $NADP^+$/NADPH can serve as a pool of net two electrons or a hydride ion. The absence of quenching of luminescence of of $Ru(bipy)_3^{2+}$ by 1 M BNA or 1 M triethyl amine, suggests that the photosensitized reactions do not invlove any interactions of Ru $(bipy)_3^{2+}$ in the luminescent excited state with either BNA^+ or the amines. A non-emmissive state of $Ru(bipy)_3^2$ appears to be involved.
2.	RuL_3^{2+} L = [bipyridyl-pyrimidine structure with R_1, R_2] R_1 = H; R_2 = H R_1 = CH_3; R_2 = H R_1 = H; R_2 = Phenyl L = [pyridyl-pyrimidine structure with R] R = CH_3; R = Ph	MV^{2+}	Triethanol amine	To find out relations between photophysical properties and photocatalytic abilities. All the complexes show metal to ligand charge transfer absorption and emission around 450-500 nm and 600-700 nm respectively. Excited state life times also measured (depends on temperature and solvent) Quantum yields of MV^+formation depends upon L, solvent. Photosensitilizer efficiencies are not explainable only by redox potentials of the excited state and life times. Slight modification

TABLE - V

	Sensitizer	Relay	Redox System	Remarks
	L = (N, N)			of ligand structure affects the mechanism of electron transfer as well as the Ru L_3^+ -solvent interactions.
	L = (N, N, N, N)			
	L = (N—N, N—N)			
	L = (N, N)			
	(Kawanishi et al, Japan)			
3.	Colloidal Prussian Blue + $Ru(bipy)_3^{2+}$ (Kaneko & Yamada, Japan)		Water → H_2 + O_2	Both the excitations of the Ru & Fe complex were needed (λ_{max} = 700 nm). Stern - Volmer plot of quenching of $Ru(bipy)_3$ by Prussian Blue shows that only static quenching occurs in this system ; S-V plots at higher concentractions of Prussian Blue shows complex formation between the two, possibly adsorption of Ru complex by colloidal Prussian Blue.
4.	Sn(II)-co-ordinated Ru & Ir complexes (Yamakawa et al, Japan)		2-propanol → acetone + hydrogen $\Delta H°$ = 100.4 KJ/mole $\Delta G°$ = 13.4 KJ/mole	Catalyst activity enhanced under photoradiation for both Ir-Sn &: Ru-Sn complex. Photoabsorption at CT band (~254 nm) found more effective.

TABLE - V

	Sensitizer	Relay	Redox System	Remarks
5.	a) $Ru(bipy)_3^{2+}$ b) Tris (2, 2'-bipyrazine)-Ru (II) complex (Kitamura et al, Japan)	Methyl viologen triethanolamine (TEOA)	$H^+ + CO_2 \rightarrow$ formic acid	a) quantum yield = 0.01 b) quantum yield = 0.05 In both cases above, TEOA was necessary for CO_2 reduction. TEOA did not yield the formic acid. It is suggested that reduction of CO_2 occurs at a lower potential in presence of TEOA because of formation of a complex $CO_2 + H_2O + NR_3 \rightarrow HO\ CO_2NHR_3$.
			$CO_2 \rightarrow$ photocarboxy - lation of aromatic hydrocarbons	Most reactive is phenanthrene. Hydrogen donors such as dihydrophenanthrene, dihydroanthracene increase quantum yield. Proton donors such as secondary and primary amines decrease quantum yield. Under optimum conditions quantum yield is 0.20 with 80% going over to 9, 10 dihydrophenanthrene-9 carboxylic acid.
6.	2, 2-Bipyridine and o-phenanthroline complexes of Ru^{2+}, Ce^{2+}, Ir^{3+} and Cr^{3+} ions (Matage et al, Japan)		Various donors studied: N, N, N', - tetra-methyl-p-phenylene NN'-diphenyl-p-phenylene diamine N, N, N', N'-tetra-methyl benzidine 3,3'-dimethylbenzidine phenothazine β-naphthylamine p-anisidine N, N'-dimethyl aniline Propyl viologen sulfonate	Picosecond laser photolysis study of radical yields $Ru(bipy)_3^{2+}$ & $Ru(phen)_3^{2+}$ -radical yields in the electron transfer quenching with various donors are approximately unity. It is less for Os & Ir complexes. In these cases radical yields are almost independent of donors. In $Cr^3(bipy)_3^{3+}$ radical yields are strongly dependent upon donors. Also life time of geminate radical pair has been measured.

TABLE - V

	Sensitizer	Relay	Redox System	Remarks
7.	$Rh(bipy)_3^{3+}$ (UV light $\lambda > 260nm$) Hubesh & Mahieu, Belgium)		dextrose $\rightarrow H_2$	Model for disposal of industrial waste and otherwise worthless biochemicals. Effect of pH & addition of TiO_2 supported Pt(O) studied. Maximum efficiency occurs at pH 1.30 and with addition of heterogeneous catalyst. Efficiency also studied as a function of the molecular weight of the carbohydrate
8.	Cyclometallated complexes - of Ir(III) & Rh (III) - Dichloro bridged dimers $[M(L)_2Cl]_2$ where L = 2-phenyl pyridine or benzoquinoline & M is Ru(III) & Ir (III) (Sprouse et al, USA)			X-ray indicates that enantiomers with M-Cl bonds trans to M-Cl bonds are formed preferentially to the mesoisomer. Only emission spectral data and luminescence life times are found. These ligands are considerably higher than 2,2'-bipyridine and 1,10 phenanthroline in the spectrochemical series; they induce lower charge transfer transitions.
9.	$[Ir(bpy)_2(C, Nbpy)(H_2O)^{3+}]$ (Rabani et al, Israel)		Br^- and oxygen in aqueous solution $3Br^- + O_2 + 2H^+ \rightarrow H_2O_2 + Br_3^-$	Photolysis at near UV and Visible wavelengths.
10.	Riboflavine phenoxazine & porphyrin (meso-tetra-meta-N-methylpridyl porphyrin zinc choloride) (Takakubo, Le Roux et al, France)		Metal complexes of Fe, Cr, Co in aqueous solution	Dye-sensitization-primary process studied by nano-second laser technique.

TABLE - V

Sensitizer	Relay	Redox System	Remarks
11. Ferrocene (four ferrocenes) (Akiyama et al, Japan)	Methylviologen in the presence of triethanolamine	-	Quantum yield for the formation of radical MV^{+} measured at 355 nm, ϕ, is nearly the same value (0.05) for (b) as for Ru $(bpy)_3Cl_2$. For (a) it is 0.02 and (c) and (d) are not effective. At 440 nm, ϕ, is very small for a, c and d whereas it is .06 for Ru $(bpy)_3Cl_2$.
12. Isopolytungstate such as $W_7O_{24}^{6-}$ and $W_{10}O_{32}^{4-}$ with and without heterogenous catalysts investigated earlier. Extended to heteropolymetallates		alcohols $\longrightarrow H_2$	$K_5BW_{12}O_{40}$ exhibits strong CT (from Oxygen to W^{VI}) spectrum at 255 nm. Exposure of aqueous methanolic solution (pH=6) leads to photoredox reaction with CH_3OH and one electron reduction species of $BW_{12}O_{40}^{5-}$ (esr). Formaldehyde and H_2 appear.
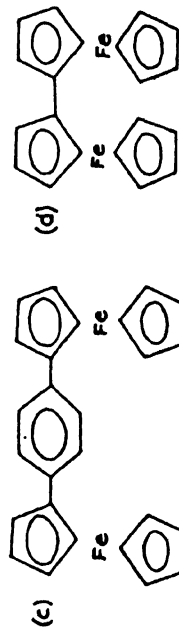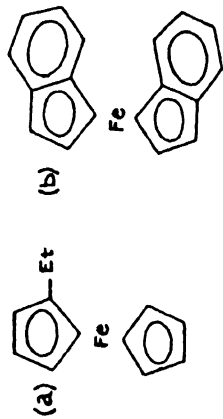
TABLE - V

	Sensitizer	Relay	Redox System	Remarks
	such as dodecatungsto borate $BW_{12}O_{40}^{5-}$ (Keggin structure co-ordination) (Yamase and Watanabe, Japan)			ϕ_{HCHO} is constant at 0.025 during photolysis and ϕ_{H_2} increases with duration of the photolysis and reaches a limiting value of 0.020. Electrical conductivity of solution increases during photolysis and remains so even after removal of irradiation (ascribable to formation of H^+ions; pH also lowers to 4.5).
13.	Zinc meso-tetraphenyl porphyrintrisulfonate (ZnTPPS) (Aono et al, Japan)	Bipyridinium salts instead of methyl-viologen	Mercaptoethanol in presence of hydrogenase	Excess amount of hydrogenase used to keep the electron transfer step to the relay as the rate determining step. Hydrogen evolution rate with C, D, E were much greater than the one with methyl-viologen. Rates do not always follow the order of the redox potentials of the compounds. The rate difference seems to depend upon the recombination rate of the separated ion pairs (determined by laser flash photolysis).

$H_3C-\overset{+}{N}$ ... $\overset{+}{N}-CH_3$ (R)

A : R = H (-0.44 eV)

B : R = CH_3 (-0.50 eV)

c) H_3C $\overset{+}{N}$ ... $\overset{+}{N}$ CH_3 (-0.72 eV)

N^+ ... N^+ $(CH_2)_n$
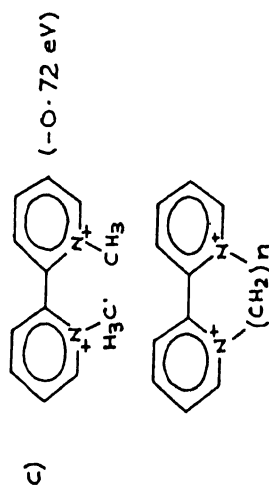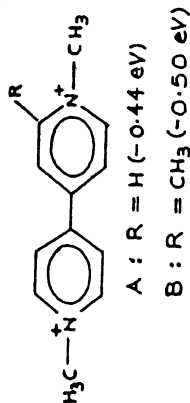
D : n = 3 (-0.55 eV)

E : n = 4 (-0.65 eV)

TABLE - V

	Sensitizer	Relay	Redox System	Remarks
14.	Zinc tetrakis (sulphonatophenyl) porphyrin ($Zn^{+}PPS^{4-}$) τ singlet=1.7 ns, τ triplet=1.40 ms (Laser photolysis) (Nahor & Rabani, Israel)	Nitrobenzene reacts with singlet		Nitrobenzene has a netural charge and its reduced form has a negative charge, therefore may be more useful for photoreduction of negatively charged photo-sensitiers. Studies in progress.
15.	Tetra 2-3 pyridino Zn porphyrazine (soluble in $DMSO_4$ not in water) (de Backer et al, France)	CO_2 in DMSO		CO_2 is soluble ten times more in DMSO than water. Cyclicvoltametry used to study the interaction of the dye and of the electrode (Pt disk) in the presence of CO_2 to determine the relative importance of the catalytic photochemical and electrochemical pro-cess. Results provide evidence for the catalysis role of phthalocyanine-types in the reduction of CO_2.
16.	Pulsed radiolysis studies (McAskill, Australia)	Methyl viologens 1,1',3',3' tetra methyl viologen^{2+}; hexamethyl viologen^{2+}; 1,1',2,2' tetra-methyl viologen^{2+};		Search for more effective electron relays. Efficiency of hydrogen production is decreased by the loss of methyl viologen from the system by a Pt-catalysed hydrogenation reaction. Pulsed radiolysis studies show that H atoms may react with these violgens by 3 mechanisms; electron transfer to give the radical cation; addition to the aromatic ring to give an adduct radical and by abstraction at one of the methyl groups to give a hydrogen deficient (benzylic)

TABLE - V

	Sensitizer	Relay	Redox System	Remarks
				radical. It is found increased instability of the methyl viologen is associated with the increased formation of the radical cation and the adduct radical. The hydrogen deficient radical could however add an H atom to reform the viologen molecule and hence reduce the loss of viologen.
17.	Anthraquinone-2-sulphonate (AQS) (Wakisaka et al, Japan)	Methyl viologen	Aqueous 2-propanol under Argon atmosphere	Irradiated with 360±30 nm light from 500 W Xenon lamp. At $pH < 5$ dihydroxyanthracene sulphonate ($AQSH_2$) was found and no reduction of MV^{2+} occured. The $AQSH_2$ formation would be probably through disproportionation of $AQSH^{\bullet}$ arising from H-atom abstraction of excited AQS from 2-propanol. At $pH > 6$, $MV^{\dot{+}}$ formed.
18.	Eosin Y (Wakisaka et al, Japan)		Duroquinone and sodium anthraquinone-2-sulfonate (AQS) in aqueous solution (2-propanol : water = 1:1) containing triethanolamine	Radical anions of quinone formed by the electron transfer between EosinY in the excited state and the quinones.
19.	$Ru(bipy)_3^{2+}$ (Tinnemans et al, the Netherlands)	Tetraza aromatic Co(II) mediator	Ascorbate	H_2& CO formed. No H_2& CO in the absence of relay. Turnover numbers of Co catalyst is 100-550,'studied by cyclic voltammetry and controlledt potential coulometry in various solvents.

TABLE - V

Sensitizer	Relay	Redox System	Remarks
20. $Co(Sep)^{3+}$ I^- (Balzani et al, Italy)	-	-	$Co(Sep)^{3+}$ can give ion-pairs with a variety of anions. $Co(Sep)^{3+} + I^- \longrightarrow Co(Sep)^{3+} \cdot I^-$; $Co(Sep)^{3+}I^- \xrightarrow{h\nu} Co(Sep)^{2+} \cdot I \longrightarrow 1/2\ I_2 + Co(Sep)^{2+}$; $Co(Sep)^{2+} + H^+ + 1/4\ O_2 \longrightarrow 1/2\ H_2O + Co(Sep)^{3+}$. Sensitizes the photo assisted oxcidation of I^- to I_2 and the photoreduction of water using oxalate ions as sacrificial agents.
21. Eu(III) at 254 nm $EuCl_3 \cdot 6H_2O$ (Ishida et al, Japan)	-	Alcohlic solution of - methyl styrene (MS) & $EuCl_3 \cdot 6H_2O$ saturated with N_2 irradiated with a high pressure Hg lamp	Dimer of MS & a 2:1 adduct of MS with the respective alcohol; also H_2 formation observed. Rate of formation of H_2 increased after MS was consumed and the turnover number reached 250 at 20 hrs. Similar reaction with styrene 1, 1-diphenyl ethylene. Effects of alocohol and deuterium labelling suggest:

TABLE - V
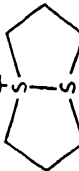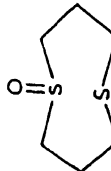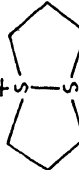
	Sensitizer	Relay	Redox System	Remarks
22.	Proflavine Thianine Benzophenone (Jones, USA)	1,5-dithiacylo octane (1) facile 2 electronoxidation to give a dication	Dication (2) + H_2O $\longrightarrow$ a stable sulfoxide (3) oxidises reversible at pH$\sim$2.	Studied by laser flash photolysis; benzophenoneketyl and radical ion (4) were implicated using laser flash techniques. The sensitized photoxidation of 1 by di-oxygen (eg. $\emptyset$ = 0.3 with benzophenone sensitizer, 80% nitrile, water). Benzophenoneketyl is absent in the presence of oxygen but 4 remains with a half life of (ca 20μs). In the presence of I^-ion, benzophenone quenched by 1 proceeds to 3 & benzophenonepinacol. With both I^- and O_2 present chemistry is very different. $1+O_2+H_2+H_2O \xrightarrow{2h\nu} 3+H_2O_2$; $4HI+O_2 \xrightarrow{2h\nu} 2I_2+2H_2O$
	1	2	3	4
23.	Proflavine, Ir $[(bpy)_2 (N,bpy) H_2O]^{3+}$ These are quenched by TMeOB at nearly diffusion - controlled rates (Brandeis et al, Israel)	Alkoxybenzenes are good electron donors and may act as quenchers. 1,4 dimethoxybenzene (DMeOB) and 1,2,4,5 tetramethoxybenzene (TMeOB) $\longrightarrow$ suitable as positive hole relays ;		$TMeOB^+$ radical studied by pulsed radiolysis techniques. Its absorption spectrum has been measured. In the presence of RuO_2 dimerization of $TMeOB^+$ occurs.

TABLE - V

	Sensitizer	Relay	Redox System	Remarks
		high redox potentials, relatively high solubilities in water and produce relatively stable cation radicals		
24.	9, 10 dicyano anthracene (DCA) (Mizuno, Japan)		1, 2 diarylcyclopropanes. The following have been observed with different diarylcyclopropanes a)($4\pi + 2\sigma$) photo-addition (85% yield) (degassed CH_3CN) b) Cis-trans photo-isomerization (aerated CH_3CN solution) c) Photooxygenation	An efficient method for charge separation between anion and cation radicals by preventing a back electron transfer from the latter to the former in homogenenous solution under sunlight radiation.
25.	$[Co(NH_3)_4CO_3]^+$ complex + $h\nu$ $\rightarrow Co^2 + 4NH_3 + CO_3^-$ (Ramakrishnan et al, India)		Tertiary cylic amines 1, 4 diazabicyclo (2,2,2) octane (DABCO); 1,3,6,8-tetraza tricycle (4,4,1.1) dodecane (TATCD); and hexamethylenetetramine (HMT)	Flash photolysis done and it suggests CO_3^- +DABCO CO_3^{2-} + $DABCO^{+}$; TATCD gives similar $TATCD^+$ but HMT gives no such intermediates. No intermediates formed in the absence of CO_3^- radical and hence direct photolysis of amines ruled out.

TABLE - V

	Sensitizer	Relay	Redox System	Remarks
26.	N,N'-1, 3 propano indigo (A) in the presence of triethylamine (T) (Setsune et al, Japan)			Photochemistry studied. $A + HD :\rightarrow [A^{-\bullet}/HD^{+\bullet}] \rightarrow [AH^{\bullet}/D^{\bullet}]$ $[AH^{\bullet}/D^{\bullet}] + H^+ \rightarrow AH_2 + D^+$ $D^{\bullet} + A + H^+ \rightarrow AH^{\bullet} + D^+$ $2AH \rightarrow AH_2 + A$
27.	Phenazine solution (> 360 nm) (Toki et al, Japan)		Styrene + triethylamine + $CO_2 \rightarrow$ Reduced products (also dimers) and carboxylic acids (also dimers)	Photosensitized carboxylation of styrenes $Ph\text{-}C(R^1) = CH(R^2)$ R^1 / R^2: H / H; Me / H; Ph / H; H / Me Studied and yields of the different products found, Suggests participation of a radical anion; phenazine radical anion observed.
28.	Chloranil anthraquinone phenanthraquinone benzophenone (Miyashi et al, Japan)		Methylene cyclopropanes (1) methylene cyclobutanes (2)	1^{+} and 2^{+} were generated and their reactivities studied : these provide both degenerate re-arrangement and very efficient moleular oxygen trapping.

Table VI Summary of posters presented on heterogeneous photocatalytic reactions

	Catalyst	Redox system	Remarks
1.	n-TiO_2 (powdered) photosensitized (Gratzel et al, Switzerland and Serpone, Canada)	Water $\longrightarrow$ H_2 & O_2 with TiO_2 (photosensitized)/Pt/RuO_2 $\longrightarrow$ Efficient sensitization observed	Photosensitized by irradiation of acidic (pH = 2) solutions of $RuL_3 + 2Cl^-$ (L = di-isopropyl 2, 2' - bipyridine 4, 4' - dicarboxylate) in the presence of TiO_2 at 100°C - loss of one bipyridy ligand and chemical fixation of RuL_2 at surface of TiO_2 particles through formation of Ru-O-Ti bonds. Very stable surface complexes, shifting absorbtion onset of TiO_2 beyond 600 mm.
2.	Pt/TiO_2 + Ethylene diamine tetra-acetic acid (EDTA) (Sasse et al, Australia)	Water with sacrificial donors (EDTA) Also effects of addition of sensitizers such as Ru $(bipy)_3^{2+}$ and others studied.	Without EDTA detectable amounts of H_2 were not produced. H_2 & CO_2 formation studied. Instead of EDTA, other sacrificial donors such as formaldehyde, formic acid, acetic acid were also studied. Main purpose is to study the fate of the spent donor and to establish new synthetic processes and to find new methods for degradation of water contaminants and destruction of organic waste materials.
3.	Platinized TiO_2 (500 W-Xe lamp) Pt loaded by photodecomposition (Kawai et al Japan)	Alcohols and water	Methanol + water $\longrightarrow$ H_2, HCHO, CO_2 n-propanol + H_2O $\longrightarrow$ H_2, C_2H_5CHO, $(CH_3)_2CO$, CO_2 In these 2 cases rate of production of H_2O and CO_2 increased with increase in H_2O pressure. Ethanol + H_2O $\longrightarrow$ H_2 and CH_3CHO i - propanol + H_2O $\longrightarrow$ H_2 + $(CH_3)_2CO$ Rates were independent of H_2O pressure. Effect of H_2O pressure observed for the alcohols for which the valence band position was deeper than that of H_2O adsorbate. Mechanisms proposed.

TABLE - VI

	Catalyst	Redox system	Remarks
4.	Anatase subjected to repeated sulfurization, oxidation and then loaded with Pt or Ni ; Also $SrTiO_3$ treated the same way. (Sekine) et al, Japan)	Isopropanol and water mixture, Anatase/Pt catalyst subjected to these treatments gave 21% light quantum efficiency; $SrTiO_3$/Pt, $SrTiO_3$/Ni gave 30% and 8% respectively.	Studies on Ti metal sheets with repeated oxidization, sulfurization establishes the formation of composite sulfurized and oxide compounds near the surface. The hope is that by such treatments electronic excitation of these semiconductor catalysts by visible lights may be possible.
5.	Photodeposited Pt on TiO_2 particles (0.5 to 1 μm diameter) with alcohols or carboxylic acids as sacrificial donors (Nakamatsu et al, Japan)	The hydrogen production rates using ethanol as sacrificial donor showed that there is an optimum Pt-Pt distance ($\sim$100 nm obtained with CH_3COOH as donor)	Form (size and spacing) of deposit varies with sacrificial donors; light intensity and K_2PtCl_6 concentration were only minor factors. Electron microscopic studies made. In decreasing order of size and spacing, the donors would be ordered thus : acetic acid, t-butanol, methanol, i-propanol, ethanol.
6.	M/TiO_2 photocatalyst with M = (Pd, Pt, Cu, Fe & Ni) prepared by hydrolysis of $TiCl_4$ with the corresponding transition metal (Chen Jian, China)	Dilute aqueous solution of ethanol $\longrightarrow$ acetaldehyde + H_2	H_2 comes from the reduction of H_2O rather than ethanol (Isotopic experiments of Sakata); Oxidation of ethanol is better in an open system (contact with air) than in a closed system (in Ar atmosphere)
7.	TiO_2 modified by Ion doping or metal deposition - changes surface electron concentration - n_s (Herrmann et al, France)	Cr^{3+} doped anatase - with visible light no catalytic effect and with UV catalytic effect is reduced (since Cr^{3+} ions are filled acceptor centers and attract photoproduced holes, enhancing recombination rates).	Variations in n_s, followed by measurement of photoconductors of Cr^{3+} doped TiO_2, without changing particle size and shape, absorption spectrum from UV to visible but photoconductance drops by 10^3 with no change in energy gap. This study shows that modifications, whose aim is to improve surface properties or to change the photoconductivity of a semiconductor can

TABLE - VI

	Catalyst	Redox system	Remarks
		Oxidation of 2-propanol propene, oxalic acid (aqueous solution) studied. For Pt, Rh Ni doped TiO_2, low doping metal percentage has beneficial effect. Beyond an optimal metal content, effect is non-beneficial. (In these cases, studies made on deuterium-cycloopentane isotopic exchange, alcohol dehydrogenation and for oxygen isotope hetero exchange).	affect the surface electron density of this solid and consequently perturb its photocatalytic activity.
8.	Aqueous suspensions of TiO_2/Pt (powdered mixture of anatase TiO_2 with Pt black) (Ohtani et al, Japan)	Primary monoamines and diamines $\longrightarrow$ cyclic and a cyclic secondary amines; (eg) $CH_3CH_2NH_2 \longrightarrow$ $(CH_3CH_2)_2NH$ in aqueous solution. At basic pH dipropylamine yield decreased and propionaldehyde yield increased In acetonitrile, n-propylidenepropylamine was obtained.	Rate of conversion was negligibly small with TiO_2 or Pt alone when irradiated. Present method seems to be favourable for intramolecular conversion of primary amines to cyclic secondary amines.
9.	Aqueous suspensions of TiO_2 (Muraki et al, Japan)	$H_2O \longrightarrow H_2O_2$ By comparing cyclic voltammograms with the special electrode and the photocurrents with the same electrode, this reaction has been	It is established by cyclic voltammetry with optically transparent electrode whose surface was chemically modified with n-dodecyltri-ethoxysilane that the main hole reaction is $2h^+ + 2OH^- \longrightarrow H_2O_2$ This electrode can detect H_2O_2 or O_2 independently.

TABLE - VI

	Catalyst	Redox system	Remarks
		established as the first step in the photo-oxidation of water.	
10.	Pt/TiO_2	a) Methanol and water vapour to hydrogen and HCHO - vapour phase reaction efficiency is an order of magnitude smaller than in liquid phase. Methanol water vapour mixture is more efficient than methanol alone in vapour phase (the other way in liquid phase)	N_2 fixation and hydrogen production studied in vapour phase using pulsed laser dynamic mass spectroscopic technique.
	Fe/TiO_2 (Hashimoto and Sakata, Japan)	b) N_2 gas and water vapour $\longrightarrow$ NH_3 only if Fe was present. In liquid phase Fe/TiO_2 shows best yield until now and alkaline pH is better. Vapour phase gives more yield than liquid phase.	
11.	a) Unloaded TiO_2 with adsorbed water b) Pt loaded TiO_2 (Anpo et al, Japan)	Alkyne or Alkene $\longrightarrow$ CO_2, CO, CH_4, C_2H_4, C_2H_6, C_3H_6 C_3H_8 with $CH_3\text{-}C \equiv CH$. With (b) a significant increase in C_3H_6 and C_3H_8 is found. With unloaded TiO_2 ESR shows Ti^{3+} on irradiation. Metal loaded TiO_2 shows no Ti^{3+} signal.	Isotope studies show that H atoms are from adsorbed H_2O molecules and not from surface OH groups. Features are explained on the basis that interaction of alkenes (or alkynes) with electrons and holes plays a significant role in photo-hydrogenation accompanied by the bond fission. The yield of photo-reaction increases with decrease of TiO_2 particle size. Selectivity also changes. λ max shifts to shorter λ with decreasing particle size of TiO_2.

TABLE - VI

	Catalyst	Redox system	Remarks
12.	Platinum carbonyl clusters $Pt_3 [(CO)_6]_4^{2-}$ on TiO_2 powder evaporated by air oxidation at room temperature or by vacuum pyrolysis at 150°C (Houlding et al, USA)	EDTA - an electron donor	Compared with catalysts made by pyrolysis of H_2PtCl_6 onto TiO_2 and with Pt° sols; catalysts prepared by vacuum pyrolysis is an order of magnitude better in efficiency compared to that prepared by the pyrolysis of an equal Pt weight of H_2PtCl_6.
13.	TiO_2 photocatalytic particles in suspension (Nakabayashi et al, Japan)	Studies on single charge accumulation dynamic by Time Domain Reflectometry, (TDR) establishes that the rate of injection of photoelectrons to the protons in the solution is slower than the rate of injection to MV^{2+} when it is present.	TDR observes the time dependence of the dielectric constant of the sample by pertubation of electric field strength.
14.	TiO_2, Pt-TiO_2 (Brugger, Switzerland Chunying et al, China)	Reduced methylviologen Conclusion : Combination of Pt & TiO_2 might create more efficient path for electron transfer.	Investigated the electron transfer process across $TiO_2/MV^{+\cdot}$ or Pt-$TiO_2/MV^{+\cdot}$ solution interface in an electrochemical cell. H_2 evolved at the electrodes in closed or open circuit conditions were measured. $MV^{+\cdot}$ in solution maintained at constant concentration by photo generation or electrochemical reduction.
15.	RuO_2-loaded CdS suspensions or CdS/Rh_2O_3 particles (Dimitrizevic, Yugoslavia Li, China; Gratzel, Switzerland)	$H_2O \longrightarrow O_2$ visible light radiation	No O_2 with bare CdS; with Rh_2O_3 initial rate of evolution of O_2 is 15 times higher with a catalyst that has two times smaller degree of loading with Rh_2O_3 than the RuO_2 catalyst.

TABLE - VI

	Catalyst	Redox system	Remarks
16.	Ru(IV) oxide catalysts (Mills and Lawrence, UK)	Oxidation of water Anodic corrosion to RuO_4	Contradicts Gratezel group's results. Anodic corrosion of $RuO_2.XH_2O$ does not dependent on [Ru IV]/[CE(IV)] ratio. Gratzel claim was that Ce(IV) stabilized Ru(IV). Establishes that Gratzel had used a mixture of $RuO_2.XH_2O$ and a partially dehydrated form with only the latter exhibiting any catalytic activity or stability toward anode corrosion.
17.	RuS_2 (loaded 0.5 wt %) deposited on CdS in alkaline aqueous suspension (Mackor et al, Netherlands)	$SO_3^{2-} + HS^- + H_2O\,(ads) \xrightarrow[h\nu]{CdS/RuS_2}$ $H_2 + S_2O_3^{2-} + HO^-$	Approximately 7 times more active than CdS/RuO_2 (0.5 wt %) Response studied as a function of wave length shows maximum at band gap energy of CdS (2.4 eV) and not at that of RuS_2. At peak value (450 nm) quantum efficiency $\sim$ 18%
18.	Nafion/CdS/Pt system (CdS & Pt impregnated Nafion membranes) (Bard, Fox et al, USA)	S^{2-} was used as a sacrificial reagent and this also served to stabilize the lattice S^{2-} against oxidation. Homogeneous distribution of Pt throughout the Nafion film via reduction of Pt $(NH_3)_2I_2$ by $NaBH_4 \longrightarrow$ most efficient H_2 catalyst (because of smaller average CdS-Pt separation)	Varied platinization type, CdS crystal type and irradiation wavelength and intensity. β-CdS (cubic) is more efficient and reproducible in H_2 production than α-CdS (hexagonal) (almost a factor of 3). Also β-CdS activity is regenerated after prolonged irradiation by washing the Nafion/β-CdS with hot water. When Nafion/CdS/Sputtered Pt was irradiated from Pt side the rate of H_2 production was near the short wave-length limit even for wavelengths that are weakly absorbed, implying that either excitation or charge can be transported a significant distance in these systems.
19.	CdS particles, monograin membranes and single crystals	Suspensions : RuO_2 loaded or RuO_2 + Pt loaded particles gave no O_2 but only H_2	H_2 production for pH > 7 for 15 hours; after 15 hours pH $\sim$ 5 and H_2 production stopped. Adjustment of pH to a higher value leads to further H_2 evolution.

TABLE - VI

	Catalyst	Redox system	Remarks
	(Memming et al, W. Germany)		Formation of sulfate ion is responsible for change of pH. Conclusion is that in aerated solutions CdS is not stable.
20.	Platinized CdS powder Best catalyst obtained so far is that from hexagonal CdS powder annealed at 800°C in a nitrogen atmosphere and loaded with 2% Pt powder by the shaking method. Quantum efficiency from 436 nm to 480 nm ~ 28% / 35°C dropped to zero at $\lambda >$ 550 nm; 33% at 60°C For AM1 H_2 evolution was 0.32 mol (7.2 l) $m^{-2}h^{-1}$ at 35°C and 0.51 mol (11.4 l) $m^{-2}h^{-1}$ at 70°C) Catalyst was durable (no change in weight or catalytic activity at least for 27 hours with 1.0 M Na_2SO_4 solution purged with nitrogen; during this time solution was	Aqueous solution of sulfite : 1 M Na_2SO_3 buffered at pH ~ 8.7	1) Hexagonal CdS is more efficient as a photocatalyst than cubic CdS 2) Three methods of preparation of catalyst used (a) grinding CdS & Pt black powder (efficiency decreased with increase of grinding time) ground powder shows enhanced photoabsorption at wavelengths longer than band gap excitation showing that recombination centres are generated by grinding - this decreased efficiency. (b) Photodeposition of Pt on CdS from aqueous solution of H_2PtCl_6 (c) CdS powder loaded with Pt powder by shaking in a glass vessel and this catalyst showed the highest efficiency.

TABLE - VI

	Catalyst	Redox system	Remarks
	changed 6 times to maintain concentration and pH (Tsubomora et al, Japan)		
21.	CdS, Se (modified) (Kawai et al, Japan)	1) aqueous Na_2SO_3	1) Photocatalytic H_2 production rate is controlled by the S-concentration at the Cd(S, Se) surface. XPS shows surface concentration of S is different from that of the bulk.
		2) aqueous ethanol	2) Oxidation of CdS or CdSe surface at 550°C for 5 minutes dramatically increases activity; oxidation was most effective for a short period (30 sec). XPS shows surface of the most active CdSe was covered by a very thin oxygen layer.
		3) Photoasymmetric synthesis : Methylaceate + H_2 gas (1 atm) $\xrightarrow[\text{Temp}]{\text{Room}}$ optically active 3-hydroxybutyrate	3) Using CdS with asymmetrically modified Raney Ni (This reaction occurs with Raney Ni alone at 100°C and 100 atm pressure)
22.	Thin films of CdS & TiO_2 on quartz substrate (RF sputtering). Pt deposition on TiO_2 increased activity 50 to 200 fold (both photo deposition and electroless reduction gave	Watermethanol mixture $\longrightarrow$ H_2 and CO_2	For TiO_2 sputtering in Ar atmosphere gave higher yield of H_2 than when sputtered in O_2 atmosphere (related to oxygen deficiencies produced in TiO_2 films during sputtering). For CdS, H_2 generation linearly increased with film thickness (0 to 5 μm). Also lower rf power density for sputtering increased photocatalytic activity, X-ray analysis shows that crystallinity was an important factor and that when C-axis orientation of crystal was increased, photocatalytic activity

TABLE - VI

	Catalyst	Redox system	Remarks
	similar effects). Back irradiation (from quartz side, possibly due to greater photoabsorption, gave better activity than front irradiation (Pt side) (Nakayama et al, Japan)		increased.
23.	ZnO powder suspended in an aqueous solution containing $AgClO_4$ and KNO_3 (photo reduction of Ag^+) (Yonezawa et al, Japan)	a) Uranine (10^{-5}M) added to photosensitize b) 2-propanol added instead of Uranine	a) With ZnO alone photo reduction of Ag^+ occurs at 365 nm. ϕ_{Ag} = 0.21. With uranine - $AgClO_4$ solution but no ZnO, ϕ_{Ag} = 0.0001 with 500 nm; with ZnO — Uranine, ϕ_{Ag} = 0.02 with 500 nm. b) ϕ_{Ag} = 0.45
24.	Xanthene sensitized ZnO/Pt photocatalyst for visible light induced water reduction (also applicable to photoreduction of CO_2, N_2, organic compounds, etc.) (Koide et al, Japan)	a) Rose Bengal (halogenated) as sensitizer b) Uranine (non-halogenated) c) I^- added to uranine	a) $\phi >$ 20% but tends to photodehalogenate b) $\phi >$ 3% but photodurable c) $\phi >$ 22% at 492 nm with no photodeterioration (Heavy atom effect) Br^-, Cs^+ and Xe also increase rate; effect was proportional to square of spin-orbit coupling constants. (Reductive electron transfer mechanism through T_1 states of the dye is proposed).

TABLE - VI

	Catalyst	Redox system	Remarks
25.	Untreated non-metalized ZnS (Ishimaru et al, Japan)	Primary amines to secondary amines	λ >290 nm (High pressure Hg)
26.	ZnS generated by UV irridiation of metal dithiolenes (Kisch et al, W. Germany)	With aqueous solution of tetrahydro-furan or 2, 5-dihyrofuran hydrogen evolution and dehydrodimerization of cyclic ether.	Maximum turnover number = 2000 - 4000 mol H_2/mol ZnS ϕ 300 nm $\geq$ 0.1
27.	ZnS dispersed aqueous solution of organic substrates (Midori et al, Japan)	Dihydrofurans, cyclopentene, cyclohexene, 2-methylfuran, ethylbenzenes and toluene $\longrightarrow$ H_2 & dimeric products coupled at benzyl or allylic carbons and/or oligomers.	A heterogeneous three phase-substrate, water and ZnS
28.	V_2O_5, V_2O_4 aqueous dispersion loaded with RuO_2 and Pt (Namari et al, Iraq)	Water-Electron relays such as MV^{2+} and EDTA and different buffer solutions tried - complexes and a number of oxides and oxyhydroxides formed.	Inefficient and not reproducible.
29.	Aqueous dispersion of Ag^+ zeolites initially insensitive to invisible light become photoactive after having them illuminated for a few minutes of light of	At acid pH, in presence of Cl^- ions, chlorine production occurs. At neutral or alkaline pH, oxygen production occurs.	Most probably silver atoms initially and silver clusters later on are formed.

TABLE - VI

	Catalyst	Redox system	Remarks
	higher energy (Calzaferri et al, Switzerland)		
30.	a) Photoinduced current and H_2 production found to be correlated in TiO_2; TiO_2/Ag; TiO_2/Pt and CaS/Pt	Ethanol (pH 7) HCOO Na (pH 9) Ethanol (7) Ethanol (14) NaS_2 (13)	Maximum current of 12 mA (quantum yield 30%) with CdS/Pt aqueous ethanol with pH =14, when inadiated with visible light.
	b) Photoelectrochromism (Photointercalation accompanying the colour change)	WO_3/aqueous ethanol - dark green on irradiation. WO_3/aqueous formic acid - dark green on irradiation. WO_3/Pt in aqueous formic acid - green changing to deep blue on irradiation.	Possible application in information storage using light signals.
	c) Synthesis of amino acid; In_2O_3, $SrTiO_3$ TiO_2 or Fe_2O_3 as a photocatalyst. (S. Kawai,et al, Japan)	C_2H_5 COOH and aqueous ammonia $\longrightarrow$ alanine; yield of alanine increased with the increase in depth of the valence band positions.	Experiments suggest that formation of radicals $CH_3CHCOOH$ and NH_2 can lead to alanine.
31.	TiO_2, CdS, CdSe & MoS_2 were used either with or without Pt deposition	50 m mol of glucose or an organic acid, 50 m mol of NH_3 or NH_4Cl and 300 mg of photocatalyst powder in 30 ml water -	Glucose-ammonia $\xrightarrow[CdS/Pt]{TiO_2/Pt}$ mainly glycine with CdS/Pt alanine and serine. With TiO_2 (unloaded) mainly glycine. Organic acid-ammonia CdS/Pt $\longrightarrow$: alanine from pyruvic

	Catalyst	Redox system	Remarks
	(T. Kawai and S. Kawai, Japan)	irradiated by a 500 W Xe lamp for 10 hours.	acid; aspartic acid from fumaric acid or oxaloacetic acid; glutamic acid from ketoglutaric acid. (quantum yields from 3 to 35%) Peptides can also be produced - glycyl glycine and oligopeptide from aqueous glycine solution and also from glucose-ammonia system with CdS/Pt.
32.	Freshly prepared ZnS, CdS or commercial TiO_2 (0.1 m mol) in 10 ml methanol - for photo-sensitized isomerization (Also effective is an organic semi-conductor, poly p-phenylene) (Mizumoto et al, Japan)	Ester (0.04 M) irradiated at λ >290 nm with stirring.	Photosensitized isomerization of methyl oleate (cis ester) and methyl elaidate (trans ester) ZnS & CdS are as effective as some triplet sensitizers for this isomerization (such as acetone, benzil) but TiO_2 did not sensitize.
33.	TiO_2 (anatase and rutile), $SrTiO_3$, $BaTiO_3$, CdS, Fe_2O_3 and ZnO ⟶ Metallized with Pt, Rh, and Pd. (Sato & Yamaguti, Japan)	Gas phase (with NaOH coated catalyst) water photolysis	Activity sequence is anatase $>$ rutile $>$ $SrTiO_3$ and for metals loaded Rh $>$ Pt $>$ Pd. Rest were not active.
34.	n-TiO_2, n-Fe_2O_3, n-WO_3, p-Cu_2O semiconductor	TiO_2, Fe_2O_3 and WO_3 colloids flat band potentials were within 100	Flat band potentials determined by pulse radiolysis. For TiO_2 and Fe_2O_3 flat band potentials were independent of

TABLE - VI

	Catalyst	Redox system	Remarks
	colloids (Nozik et al, USA)	to 200 mV of values for compact semiconductor electrodes. For p-Cu_2O it was 1 volt more negative than that of the compact electrode. For particle sizes below 50-100 A° size quantization effects become evident.	size over 70 A° to 800 A° diameter range. Mössbauer spectroscopy of Fe^{3+} ions in frozen solutions to study kinetics of charge transfer from illuminated TiO_2 and CdS semiconductor slurries and colloids.
35.	Oxobridged bipyridyl system $\left[(bpy)_2 Ru^{III}(OH_2) - O - Ru^{III}(OH_2)(bpy)_2\right]^{4+}$ immobilized on 200 A° diameter colloidal silica support (Frank, USA and Honda and Kondo, Japan)	Water	Immobilization improved the stability of the dimer at pH 5-6; studied as a water oxidation catalyst. Turn over number (40) - stability is better when immobilized at pH 5-6.
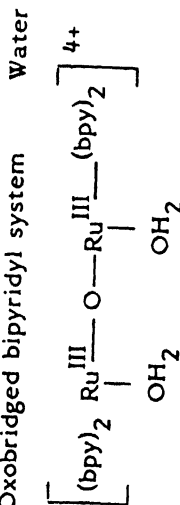
ORGANISED MOLECULAR ASSEMBLIES; SIMULATION AND MECHANISM OF PHOTOSYNTHESIS

The key to the success of any photosynthetic route, wherein the primary process after photon absorption is the creation of a charged pair, lies in the instant and efficient separation of the charged pair leading to an inhibition of the back electron transfer reaction. The separation can be achieved either by phase separation such as in microemulsions, micelles, membranes, vesicles, etc. or by incorporation of highly charged microenvironment e.g. polyelectrolyte in molecular assemblies.

Polyelectrolytes seem to be good candidates since they posses certain features : (1) a well defined structure whose properties, namely, size, shape, charge density, etc. can be modified by conventional synthetic techniques; (2) the possibility to attach specific chromophores to them such that they posses the desired properties (absorption spectra, redox potentials, solubilities etc.) (3) the capability of their attachment to electrodes and (4) the ability for adsorption or attachment of colloidal catalysts to them. Functional polyelectrolytes consisting of charged segments and photoelectrochemically active groups have been demonstrated to serve as a new class of interfacial microenvironments that effectively control the rate and direction of light-induced transfer reactions.

Rabani (Israel) reviewed the status in this fascinating subject of separation of photoredox products by local potential fields with special reference to polyelectrolyte. The sequence of events in an anionic polyelectrolyte to which a photosensitizer P and an electron acceptor Q is attached as a complex PQ, following absorption of a photon is as follows :
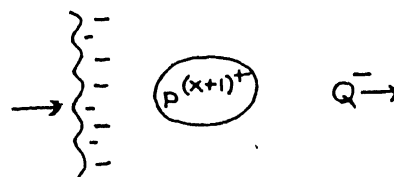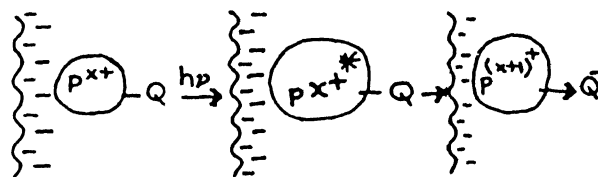
With cationic polyelectrolytes the ultimate system would be
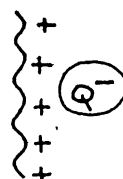
An example of such a system is P = Cis $(Ru\ bipy)_2\,(CN)_2$ and Q = $Fe(CN)_6^{3-}$

on positive charged polybrene,

$$\left[-(CH_2)_3 - \overset{CH_3}{\underset{CH_3}{N^{+}}} - (CH_2)_6 - \overset{CH_3}{\underset{CH_3}{N^{+}}} - \right]_n \cdot (F^-)_{2n}$$
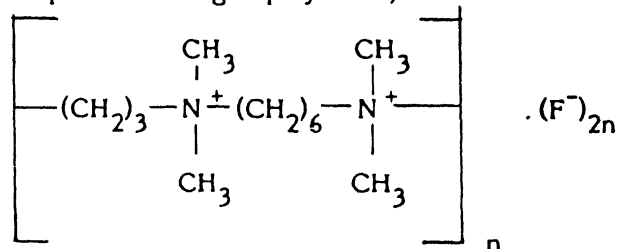
The rate of quenching by $Fe(CN)_6^{3-}$ is 40% slower in the polymer

Laser flash photolysis studies of Ru $(bipy)_2 (CN)_2$ - $Fe(CN)^{3-}$ photoinduced electron transfer system in the presence of the positive polyelectrolyte, polybrene, indicates efficient retardation of back electron transfer. In table VII can be found the summary of posters presented on utilization of polyelectrolytes as effective charge separation media.

Matsuo (Japan) described in a plenary talk the role of organized molecular assemblies in artificial photosynthesis. For the purpose of light harvesting, various chromophores have been incorporated into surfactant molecular assemblies such as micelles, bilayer molecular membranes and liposomes. Polymers with pendant chromophores have also been investigated. In these highly crowded molecular assemblies the deactivation via excimer formation can be reduced by the use of spacer alkyl chains with appropriate length. Many novel light harvesting molecular bilayer assemblies with well defined molecular organisations, controllable molecular orientation and component distribution have been studied. The absorption characteristics depend upon the nature of aggregation. The second step of separation of the photogenerated charged redox pairs can be controlled by two entirely different ways depending on the types of electron transport processes : molecular diffusion of electron mediators (type A) or electron migration (or hopping) between the mediators (type B). Type A mechanism is the only mechanism in homogeneous system; in charge separation at the phase boundary type B becomes dominant. In both types charge separation efficiencies can be improved by use of appropriately designed molecular assemblies.

Polypyridineruthenium (II) complex - viologen pairs have been well studied for charge separation in homogenous solutions. The probability of the survival for the primary redox pairs depends upon the cage escape yield of each component. Even the cage escaped redox pairs are quickly annihilated by reverse electron transfer in a completely homogeneous solution. Such an annihilation is suppressed by trapping one of the components of the redox pair in a microenvironment (that is inaccessible to the counter part) such as a micelle. Amphipathic viologens lend themselves for formation of novel micellar systems as well as bilayer molecular membranes (See Table VII). One of the best examples is the case of bilayer membrane formed by an amphipathic viologen with two hexadecyl groups (See 18 in Table VII). The injected electron on the bilayer membrane survives for an appreciable period. Better results are obtained with Zn porphyrin complexes as sensitizer. It is clear that molecular assemblies with aligned viologen units on the surface can be used as an electron pool, which collects the photoliberated electrons and stores them for certain periods of time. Similar effects are observed with viologen polymer. The photoliberated electron from a Ru complex is transported to pendant viologen groups of the polymer via zwitterionic viologen and the life time of the reduced viologen is as high as 1.2 seconds. The trapped electron migrates along the pendant viologen groups till it is finally captured by an electron sink such as platinum colloid. Such organised molecular assemblies besides aiding charged separation provide temporary storage of chemical energy.

Studies on charge separation at the phase boundary have been made from three different aspects : (a) molecular design of photosensitizer (b) methods of charge transport in the membrane and (c) separation of longer living chemical storage products across the membranes.

Amphipathic derivatives of polypyridine Ru(II) and Zn porphyrin complexes(II) have been proved as efficient sensitizers at the boundary. However reverse electron transfer becomes a serious problem in these cases since molecular diffusion of electron mediator is difficult in viscous microenvironments. To get around this difficulty the photoliberated electron is transported without disturbing the molecular alignment, by the use of amphipathic viologen molecular assemblies, where electron migration (or hopping) is possible due to the exchange between the adjacent viologen units. Such electron migration in biomembrane model system is capable of even competing with intramolecular reverse electron transfer which is inherent in covalently linked sensitizer-electron acceptor system such as

polypyridylruthenium(II) complex with linked viologen units. By coupling two photoredox systems with electron transport systems consisting of aligned viologens on the phase boundary, tandem type two photon activation has been accomplished. Some of the linked donor-acceptor system as organised molecular assemblies are also considered in Table VIII; Matsuo reported the increase of life time of the charge separated species in assemblies such as

viologen - $(CH_2)_n$ - NH - C(=O) - [bipyridine] - $Ru(bipy)_2^{3+}$

viologen - $(CH_2)_n$ - NH - C(=O) - [bipyridine]

— Sensitizer
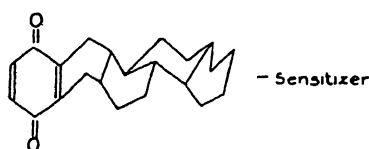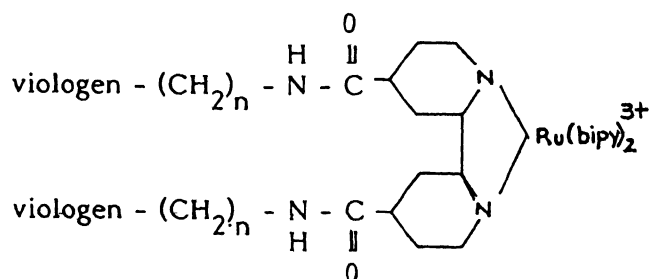
Ru complex bound to these colloidal particles have also been investigated.

A new generation of synthetic bilayer membranes have been designed for example, with those formed with

$CH_3(CH_2)_n$ CH_3

N^+

$CH_3(CH_2)_n$ CH_3
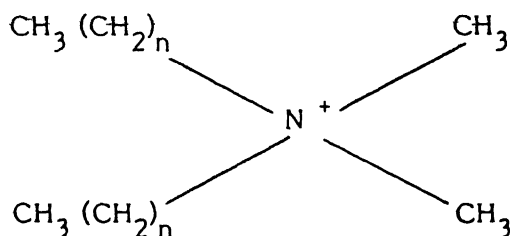
a single chain leads to a micelle and a double or triple chain gives bilayers, a single chain with rigid segments also results in a bilayer. Such bilayer films can be cast on glass plates and peeled off for use as membranes (close to achieving engineering of bilayers).

Vertical electron transport across relatively thick membrane as well as efficient catalyst for converting redox energy into useful material, remain as problems awaiting solutions in the near future. We seem to have found good guiding principles for designing organized molecular assemblies.

Tabushi, Kinnaird and Kugimiya (Japan) discussed, in their invited presentation, a multiphase liposome system. They have developed a mathematical model representing the multiphase system and have attempted at optimization so that forward reactions compete successfully with back reactions. A nearly optimized system incorporate $ZnT_{SO_3Na}PP$ (Zinc complex of tetra-(P-sodium sulfonato) phenyl porphyrin) as photosensitizer C_4V^{2+} [dibutyl-4,4'-bipyridinium] viologen as the electron carrier, $Na_2S_2O_3$ as an electron source and Flavin mononucleotide (FMN) as the electron acceptor and a bilayer single-wall liposome to separate the $Na_2S_2O_3$ from FMN reduction.
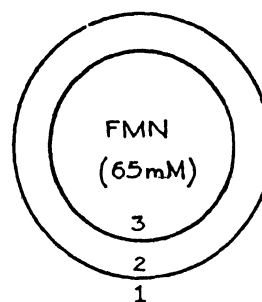
$Na_2S_2O_3$ successfully competes with the reduced viologen cation radical for oxidized photosensitizer, when appropriate concentration of each are used. As a result, the loss of photocatalyt is low and a relatively high turnover (about 120 moles of FMNH produced per $ZNT_{SO_3Na}PP$ consumed) results.

The effective competition of $Na_2S_2O_3$ for oxidized porphyrin cation radical causes a build up of viologen cation radical in aqueous phase 1, causing a flux of the viologen radical into liposomal aqueous phase 3, through the liposomal membrane (phase 2). By balancing the hydrophobicity and hydrophilicity of the dication and radical cationic viologens, it is possible to maintain appropriate rates of inward viologen cation-radical and outward viologen dication flux (this is defined as flux conjugation). Using this concept the alkyl chain length of the viologen was determined to be 4 carbons for optimization of electron carrier ability of viologen. Furthermore the rapid reduction of FMN to FMNH in the interior of the liposomes

shows that the electron-releasing aspect of the system is also near or at optimum. To further optimize this state, the primary photoevents of quenching the electron-transfer product cage escape must be studied. The photoreactivity of a series of symmetrically and unsymmetrically metallated gable porphyrins are being studied.

M1TrPP M2TrPP

a) $M_1 = M_2 = H$

b) $M_1 = H$; $M_2 = Zn^{2+}$

c) $M_1 = M_2 = Zn^{2+}$
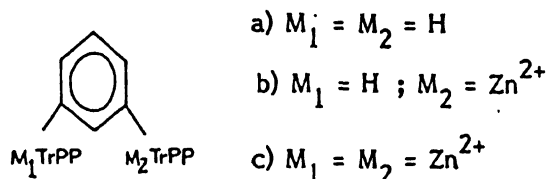
Liposomes are expected to provide an anisotropic medium for the vectoriality which is necessary for the energy storing reactions including artificial photosynthesis.

Table VIII is a summary of the several posters presented on the general subject of "Mechanism and Simulation of Photosynthesis". The synthesis of molecules which mimic the photochemistry and photophysics of the several steps of photosynthesis is of interest for two reasons : Studies of such models can reveal much about the physics and chemistry underlying natural photosynthesis; these synthetic systems can yield information which is of value for the design of artifical photosynthetic assemblages. As is seen from Table VIII much emphasis is on synthesis of coupled donor-acceptor or donor-sensitizer-acceptor systems. The innovative nature of the synthesis and the philosophy behind the attempts are quite apparent. Some molecules such as xanthene dyes, carotenes are being assembled along with sensitizers to perform an antenna function.

Gust and More (USA) described the results of their photostudies on 3 systems:

R1 R2 R3 R4

Triad 1

$R_1 = R_2 =$ —C6H4—

$R_3 =$ —HN—C(=O)—CH3 (quinone)

$R_4 =$ —NH—C(=O)— (carotenoid)

Triad 2

$R_1 =$ —C6H4—NH—C(=O)—CH2— (quinone)

$R_2 =$ —C6H4—CH3

$R_3 =$ —CH3

$R_4 =$ —NH—C(=O)— (carotenoid)

Triad 3

$R_1 =$ —C6H4—NH—C(=O)—CH2— (quinone)

$R_2 =$ —C6H4—CH3

$R_3 =$ —CH3
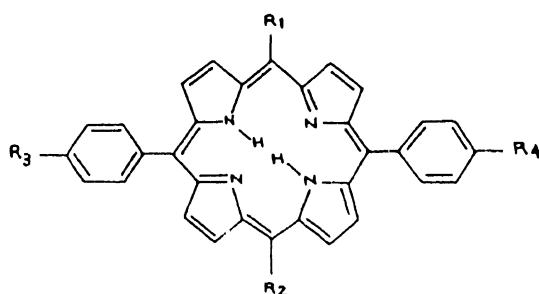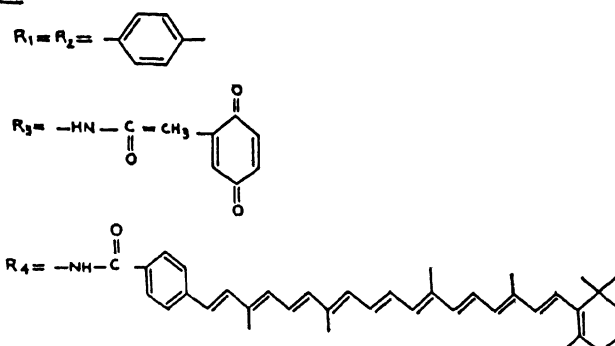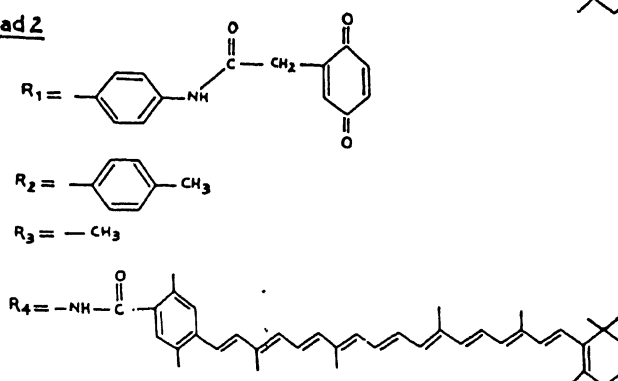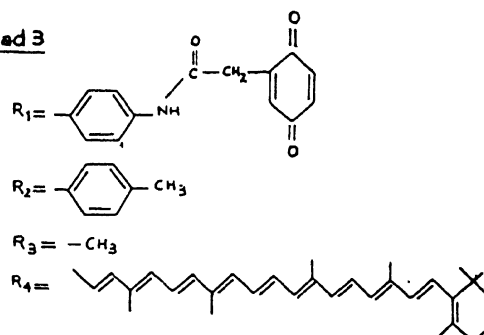
$R_4 =$ (carotenoid)

Excitation of triad 1 with a 600 nm laser pulse generates the $_1$porphyrin first excited singlet state (C - P* - Q) which donates an electron to the quinone to yield C - $P^{+\bullet}$ - $Q^{-\bullet}$. Subsequent electron transfer from carotenoid within ~100 ps of excitation gives $C^{+\bullet}$ - P - $Q^{-\bullet}$, the final charge separated state. The state is formed with a quantum yield of upto ~25% and a life time on microsecond time scale. Both the yield and life time are solvent dependent. Studies of variants such as 2 and 3 have helped define structural pre-requisites for charge separations. Triad 2 differs little from triad 1 but the charge separated state in triad 3 has a much shorter life time. Triad 1 also demonstrates

carotenoid to porphyrin singlet energy transfer (which mimics carotenoid antenna function) and porphyrin to carotenoid triplet energy transfer (which mimics natural photoprotection from singlet oxygen damage). All three carotenoid functions found in triad 1 (electron transfer, singlet energy transfer and triplet energy transfer) are desirable in solar energy coversion processes. Triads such as these can be modified to be amphipathic and incorporated into artificial photosynthetic systems. Since the length of the carotenoid moiety is ~ 30 Å these compounds may be capable of transmembrane charge conduction and photochemistry.

Norris and Gast (USA) reported the isolation of a new R. sphaeroides R-26 reaction centre single crystal. These single crystals act as compact reaction centres in a manner similar to the intact organisms. A probe of dynamics and structure that works in single crystals, in liquid or solid solutions of reaction centres, in chromatophores or in intact organisms has been developed. These single crystals can be investigated over a large temperature range with no crystal damage or loss of internal order. The ability to investigate over a large range allows one to determine important parameters, such as activation energies of the various steps and thus establish the validity of electron transfer theories in natural and artificial photosynthesis. The detailed structure and dynamical studies of a functioning, photosynthetic reaction centre complex would provide the most direct and complete bridge between natural and artificial photosynthetic systems.

At a panel discussion Kuhn (W. Germany) proposed that a tunnelling model can explain electron transfer though a barrier in between carotene and porphyrin in an organised assembly consisting of carotene porphyrinquinone. The experimentally determined equation for the electron transfer rate is

$$\ln k_{el} = a - bd - c \frac{1}{\sqrt{T}} + d\,\Delta E$$

and such an equation can be explained by an electron tunnelling model. The necessity of barriers to prevent back reaction is itself being questioned by a few workers in this field. It is expected that the following features of a molecular structure could control intramolecular electron transfer rates : (a) exergonicity, (b) conjugation, (c) nature of linkage between moieties, (d) relative orientation of moieties, (e) distance between moieties and (f) the competition between electron transfer through solvent and through bonds. Wasiewelski's rigid structures (7 in Table VIII) give the following time scales for reactions

$$DPQ \xrightarrow{h\nu} DPQ$$

$$DP^{*}Q \longrightarrow DP^{+}Q^{-} \qquad 9 \text{ ps}$$

$$DP^{+}Q^{-} \longrightarrow DPQ \qquad 180 \text{ ps}$$

$$DP^{+}Q^{-} \longrightarrow D^{+}PQ^{-} \qquad 60 \text{ ps}$$

$$D^{+}PQ^{-} \longrightarrow DPQ \qquad 2.4 \text{ s}$$
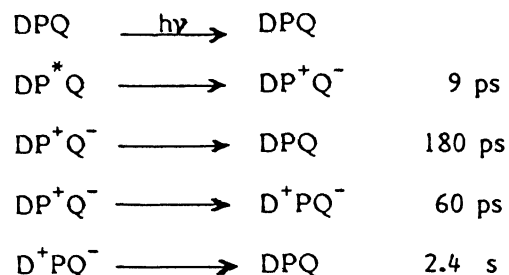
Some of these time scales are similar to those found in photosynthesis. While it was recognised that rigidity may be an important factor, over rigidity may also be counter productive.

In the attempt to use bilayer membrane (~ 40 A° thick) wherein the electron transport is reasonably fast, many questions such as procedures for obtaining a self-supporting membrane (polymer), for improving the stability of vesicles were raised. Is it possible to have molecular wires (carotenes) to conduct electron from one side of the membrane to another ? When you have a surface to which chromophores are bound how deep is the penetration of the light radiation ? Since ion transport is also necessary can we use ionopores ? It is believed that by utilising organized molecular assemblies one can achieve storage through chemical processes; generation of electricity may not be viable at all. A new area coined "Molecular electronics" may emerge. One may have an ultra thin cells with successive layers of antenna molecules, sensitizers, donor-acceptor complexes finally transferring the electrons or holes to semi-conductor/metal junction. The conduction may be through molecular wires. Such an idea is not too remote from realisation.

Table VII

Summary of posters on Photoredox Reactions and Energy Transfer in Organized Molecular Systems

A. Polyelectrolytes
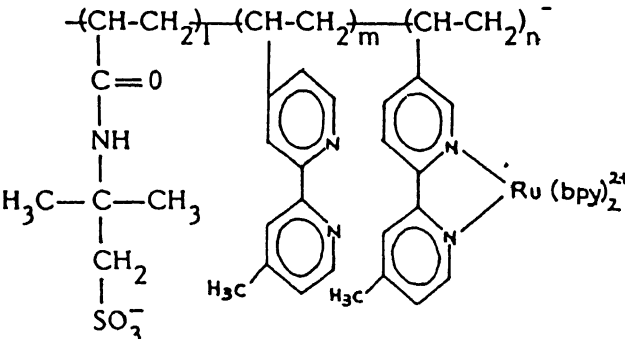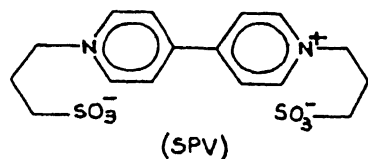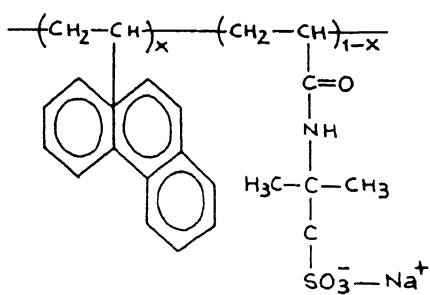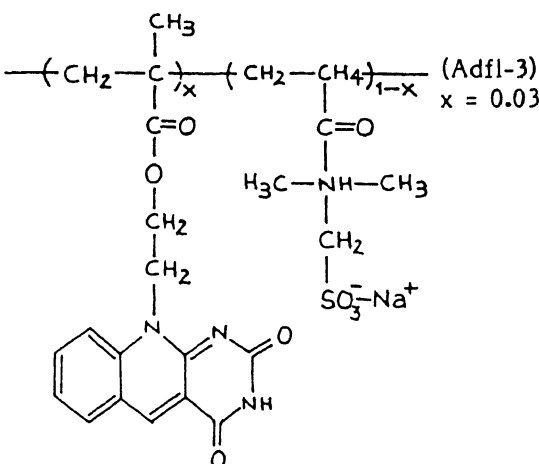
System	Remarks
1. Anionic polyelectrolyte $-(CH-CH_2)_l-(CH-CH_2)_m-(CH-CH_2)_n^-$; C=O, NH, $H_3C-C-CH_3$, CH_2, SO_3^- ; H_3C, H_3C, N, N, N, N, Ru $(bpy)_2^{2+}$	Aids charge separation of the Zwitterionic electron mediator, 1, 1'-bis (3-sulfopropyl)-4, 4' bipyridinium ; N, N^+, SO_3^-, SO_3^- (SPV)
λ max = 458, 613 nm in aqueous solution (Furue et al, Japan)	Excitation of polyelectrolyte ⟶ SPV^- and Ru^{3+} in the polyelectrolyte, (back reaction between these 2 species are inhibited).
2. The decay of polybrene radicals in the presence and absence of $Fe(CN)_6^{3-}$ (R. E. Sassoon, and J. Rabani, Israel)	Pulsed radiolysis studies. The binding of the highly charged ferricyanide ions to the polycation analysed. The decay of polybrene radicals is found to be inhibited by a jew orders of magnitude in the presence of $Fe(CN)_6^{3-}$.
3. Polyanions containing phenanthryl groups (APH-9) and 5-deazaisoalloxazine groups (AdFl - 3) ; $-(CH_2-CH)_x-(CH_2-CH)_{1-x}-$; C=O, NH, $H_3C-C-CH_3$, C, $SO_3^- - Na^+$; (APH-9) x = 0.09	Functional polyelectrolytes consisting of charged segments and photoelectro chemically active groups ; CH_3 ; $-(CH_2-C)_x-(CH_2-CH)_{1-x}-$ (Adfl-3) x = 0.03 ; C=O, O, CH_2, CH_2, N, N, O, NH, O ; C=O, $H_3C-NH-CH_3$, CH_2, $SO_3^-Na^+$

TABLE - VII
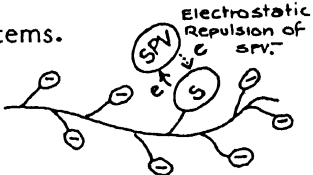
System	Remarks
The micro environmental effect was tested with the light induced reduction of methyviologen (MV^{2+}) and a Zwitterionic viologen (SPV) in aqueous systems. (Morishima et al, Japan)	MV^{+} and SPV^{-} were formed respectively; the reaction of the latter in the back reaction (reverse charge transfer) was inhibited considerably.
4. Cationic polymer containing phenanthrene (Qph-14) and anionic polymer containing 5-deazaisoalloxazine (AdFL 3) + viologen; cage escapes probability of viologen-radical ion was investigated (Ohno et el, Japan)	Study by laser photolysis kinetic spectrophotometry. $MV^{\dot{+}}$ is expected to depart rapidly from the Ph^{-} radical bound to the cationic polymer and slowly from the dFl-radical bound to the anionic polymer. SPV^{-} is expected to behave oppositely. These expectations were realized for the reactions on the ionic polymers.
5. Polyviologen polyelectrolytes	The abilities of the polyviologens to quench the emission of the lowest excited states of $Ru(bpy)_2(CN)_2$ and $Ru(bpy)_3^{2+}$ were investigated by laser flash photolysis. Highest yield of electron transfer was found for the $Ru(bpy)_3^{2+}$ - Po-XV system where the quantum yield of photo initiated electron transfer was determined to be 0.57. Higher than expected rates of quenching and back reactions are attributed to hydrophobic interactions between the bipyridine groupings of the

Electrostatic Repulsion of e^- $SPV^{\dot{-}}$

$(R-\overset{+}{N}C_5H_4-C_5H_4\overset{+}{N}-)_n\ (2Br^-)_n$ — Po-XV

R = O-xylyl $-CH_2-C_6H_4-CH_2-$ — Po-XV

R = m-xylyl — Pm-XV

R = propyl — PPrV

R = butyl — PBuV

$R_1-\overset{+}{N}C_5H_4-C_5H_4\overset{+}{N}-R_2\ (2Br^-)_{2n+1}$

$R_1 = R_2 = 2,4$, ionene = $-(\overset{+}{N}(CH_3)_2-(CH_2)_2-\overset{+}{N}(CH_3)_2-(CH_2)_4)-$ — P2,4-V

$R_1 = 2,4$, ionene $R_2 = CH_3$ — P2,4-MeV

TABLE - VII

System	Remarks
(Sassoon et al, Israel)	photosensitizer and quencher which may overcome the repulsive, coulombic forces between them.
B. Micelles and Reverse Micelles	
6. Zinc tetraphenylporphyrin in two types of reversed micelles (1) benzyl hexadecyldimethylammonium chloride (BHDC) (2) dodecyl ammonium propionate (DAP). Spectroscopic (emission and absorption) properties studied. To specify the location of the porphyrin molecule, fluoresence quenching was studied with duroquinine (resides most in the organic phase) and anthraquinone -2-sulfonate, AQS (resides mostly at the charged interface in the water pool) (Costa et al, Portugal)	In DAP a red shift (unperturbed with increase of the size of the water pool) - indicates polar head groups are in the immediate vicinity of the porphyrin chromophore. In BHDC spectra (both absorption and emission) dependent on water content-indicates a very specific micelle-chromophore interaction - possibly premicellar aggregates which are in equilibrium with a "spherical" reversėd micelle formed in the presence of water.
7. Energy transfer between cationic dyes-SDS (anionic detergent) systems (Sato et al, Japan)	Systems studied are donor-acceptor pair with closely located S_1 levels with sodium dodocyl sulfate (SDS) : Rhodamine 6G-3, 3'-diethyl-thiocarbocyanine iodate (DTC)-SDS; Rh-6G-pinacyanol-SDS; Thionine-Methylene blue-SDS. Efficiency of energy transfer was highly enhanced in these systems with peaking at the premicellar region i.e. region below critical micellar concentration of the detergent. There are 2 types of premicellar aggregates : (a) the $(D^{+}S^{-})_n$ type "salt" like aggregate (D^+ = dye cation, S-dodecyl sulfate anion and (b) dye-rich induced micelles which are a sort of micelles whose formation

TABLE - VII

System	Remarks
	is induced by addition of the dye. The peak in the energy transfer efficiency is attributed to the dye-rich induced micelles.
8. ESR & Electron Spin Echo Modulation studies of photoionization in anionic micelles. Photoproduced NNN'N'-Tetramethylbenzidine (TMB) cation in various frozen micellar and vesicle systems	ESR & ESEM allow study of structural location and water interactions of the photoproduced cation. Photoproduced cation-water interactions detected by ESEM in micelles of sodium alkyl sulfates have been found to increase with decreasing aklyl chain length. This is interpreted as consistent with asymmetric solubilization site for TMB molecule near the micellar surface and with little penetration into the micelle. In frozen alkyl sulfate solutions, the yield of photoproduced TMB^+ is found to correlate with increased TMB^+-water interactions.
Tetramethyl dodecyl sulfate (TMADS) micellar solutions compared with sodium dodecyl sulfate (SDS) micelles.	Marked increase in photoionization efficiency at 77 K which correlates with increased photoproduced cation-water interactions as determined by ESEM experiments. ESEM experiments with x-doxyl stearic acids as paramagnetic probes also indicated more water penetration in TMADS than in SDS micelles. Results are explained in terms of a decrease in the compactness of the micellar polar head group region and increased surface roughness by the substitution of more hydrophobic tetramethyl ammonium cation for sodium cation.
Addition of salt to a micellar solution results in larger micellar interface region. Photoionization of TMB in SDS anionic micelles and in dodecyl trimethyl ammonium chloride (DMC) cationic micelles studied as a function of ionic strength	Cation water interactions increase with salt solutions in both anionic and cationic micelles (maximum at about 0.2 M NaCl). Results interpreted in terms of an increase in hydration of the environment of the TMB molecule by the introduction of hydrated counterions. ESR studies

System	Remarks
using ESR & ESEM methods. (Kevan et al, USA and Pietek, Poland)	of photoionization yields of TMB at 77 K shows decrease in DTAC with salt addition and increase in SDS for salt concentrations upto 0.2 M and decrease for greater salt concentrations upto 0.5 M. Salt addition can be used to optimize charge separation for photoionized solutes in anionic micelles.
9. Photochemical behaviour of perfluorinated (F_7) anthraquinone sulfonic acid in water, cationic micellar and reversed micellar system	An irreversible electron transport from water layer in a reversed micellar system to the surrounding organic layer is already known. Hydroxide ion concentrated on the micellar surface causes an electron transfer to excited AQS trapped in micellar interface region to produce $AQS^{\dot{-}}$ Subsequent visible light radiation of $AQS^{\dot{-}}$ induced further electron transport to organic layer. However AQS is destructively oxidized by OH^-. Therefore perfluoro F_7AQS has been studied. In water photohydroxylation to α -hydroxylated F_7-AQS is observed as in the case of AQS (pH 3 ~ 11). At pH 12 average transfer complex formation between F_7 AQS and OH^- and subsequent β -hydroxylation found in dark.
F_7AQS in cationic micellar system (CTAB 6-10 mM)	Neutral pH - No photohydroxylation observed. 8-9 pH ⟶ CT complex formation between F_7 AQS and OH^- (observed) in dark.
In the presence of Cl^- photo induced formation CT complex with OH^- was considerably suppressed and photoreduction of F_7 AQS was predominantly observed.	These and other results indicate that F_7-AQS on the micellar surface has dual mode of reactions (1) photoenhanced CT formation with OH^- and (2) photoreduction by electron transfer through

System	Remarks
	the micellar surface. Efficiency of charge separation is improved by adding Cl^-
F_7 AQS in reversed micelles (Inoue et al, Japan)	In cetyl dimethylbenzyl ammonium chloride (CDBAC) reversed micelle (8×10^{-2} M) in benzene and water (1.5% V/V), no CT formation with OH^- in the dark and photoenhanced CT formation was not observed. In addition, 365 nm caused an efficient photoreduction of F_7AQS (Rate about 190 times as compared with the usual micelle under neutral conditions).
10. Efficiency of electron transfer from singlet excited pyrene to cupric ions as a function of surfactant concentration in sodium dodecyl sulfate (SDS) micelle solutions (Kira et al, Japan)	Decay of pyrene fluorescence and quantum yield of pyrene cations were increased in SDS solutions containing copper dodecyl sulfate as a quencher. Electron transfer efficiency is found to increase with the SDS concentration. Increase probably relates to increase in miceller size with probable changes in micellar structure. At higher surfactant concentration rod-like micelles dominate spherical micelles and it is hypothesized that electron transfer efficiency is higher in rod-like micelles. Addition of sodium chloride is known to increase rod-like micelles and efficiency is found to increase with addition of sodium chloride. Intersystem crossing efficiency (triplet yield) not affected by micellar concentration. It solely depended upon Cu^{2+} concentration and decreased with increase of Cu^{2+}. Thallous ions enhace triplet yield and this also was not affected by micellar concentration. This suggests that micellar size (or structure) dependence differs between an intermolecular electron transfer process and intramolecular

TABLE - VII

System	Remarks
	deactivation and intersystem crossing process.
11. Energy transfer between Rhodamine-6G and 1,3,3,1',3',3'-hexamethylindotricarbocyanine iodide (HTTC) in the presence of sodium dodecyl sulfate (SDS) studied by measuring fluorescence decay of Rh-6G. (Kasatani et al, Japan)	Time resolved energy transfer studies can reveal the location of organic molecules solubilized in micelles. The curves were simulated by an equation based on certain assumptions and models for the distribution of dyes in a micelle. The model that fits best the experimental situation is one in which the dyes distribute randomly on a micellar sphere.
12. Polymeric micelle-protected colloidal platinum (Toshima et al, Japan)	This is found to be more stable and more active than the corresponding micelle or polymer-protected colloidal Pt. The polymeric micelle-protected colloidal Pt was prepared by polymerization of the monomeric micelle-protected colloidal platinum on irradiation with ultraviolet light in the presence of $(NH_4)_2S_2O_8$ in water and further processed to produce colloidal dispersions of polymeric micelle-protected platinum. The monomeric micelle was a surfactant with a vinyl group viz. sodium undeconate. Average diameter of the colloidal particles were 11 Å System : EDTA/$Ru(bpy)^{2+}$/Methyl Viologen for H_2 from water. Activity of the polymeric micelle-protected colloidal catalyst is about twice of the corresponding anionic polymers-protected colloid.
C. Molecular Assemblies on Polymers	
13. Nylon containing pendant viologen as electron transfer mediator and matrix for stabilizing platinum. (Miyama et al, Japan)	Goal is to introduce hydrogenase into the nylon matrix containing pendant viologen groups - catalyst for photocatalystic hydrogen production from water. At the first stage, a polymer vio-

TABLE - VII

System	Remarks
	logen was synthesized.

$$-[NH(CH_2)_4\ CH\ CO]_X - [NH(CH_2)_4\ CH\ CO]_Y - [NH(CH_2)_4\ CH\ CO]_Z-$$

(X unit: side chain $N(CH_3)_2$; Y unit: side chain $N^+(CH_3)_2R$; Z unit: side chain $H_3C-N^+(CH_3)-(CH_2)_n-$ bipyridinium $-N^+-CH_3$, $3Cl^-$)

n = 4 and Y and Z were varied; R = H, C_2H_5 or $C_3H_6SO_3^-$

System	Remarks
	The efficiency of photo induced electron transfer and the ability of stabilizing Pt were examined in TEOA - $ZnTMPyP^{4+}$ - polymer viologen Pt system. It was found that the amount of hydrogen produced by the catalyst of colloidal Pt protected with polymer viologen (Z = 5, Y = 95, n = 4, R = H) was eight times larger than polyvinyl alcohol which is used frequently as a protective reagent.
14. Photochemical reactivity of pheophytin with hydrazines in plasticized polyethylene particles (Seely et al, USA)	Self quenching of excited singlet state energy can be minimized adsorbing the chlorophyll molecules to the surface of polyethylene particles which have been rendered extremely viscous by absorption of diluents such as tetradecane. To render chlorophyll strongly fluorescent it is necessary to absorb other ampiphiles with it to the particles. Chlorophyll, adsorbed to particles along with such surfactants is capable of triplet state photochemistry. Photochemistry of pheophytin contrasts with that of chlorophyll. It is easily reduced but difficult

TABLE - VII

System	Remarks
	to oxidize whereas chlorophyll is more easily oxidized than reduced. Oxidized pheophytin has a higher enough potential (+ 1.15 V) to oxidize water to oxygen. It is also more easily reduced by hydrazines than chlorophyll. This research on pheophytin has two reasons : since it is easily reduced by hydrazines use of pheophytin in the particle phase to test the accessibility of hydrazines to pigments in the particle phase; is it possible to photooxidize pheophytin to use the oxidized form for direct or indirect oxidation of water. First part has been studied and second i.e. photooxidation has not yet been successful.
15. Chlorophyll-a adsorbed with amphiphilic amides to particles of polyethylene swollen with tetradecane (refer to 14 above) (Kusumoto et al, Japan)	Amphiphilic amides : N-methyl myristamide or N-(-3 pyridyl) myristamide. A role of the amphiphilic amides is to keep adsorbed Chl in a monomeric or some associated forms which are for the most part fluorescent even at higher concentration. Spectroscopic evidence for an associated species is presented.
D. Vesicles, Bilayers, Membranes	
16. Glyceryl monoleate and phosphatidylserine BLM sensitized by a zinc tetraphenylporphyrin covalently linked to a propionic acid lateral chain, separating two aqueous media containing redox entities. This side chain not only gives to the pigments an amphipathic character (which induces an interfacial location of the chromophore but also introduces a proton exchangeable interfacial site sensitive to pH (Seta et al, France)	Coupled electron and proton transport through lipid bilayer membranes sensitized by amphipathic porphyrins. Photocurrent studied for various different values of photochemical parameters (pH, redox concentrations, light intensity). Its analysis suggests a transport mechanism which involves electron and proton transfer reactions at both interfaces.

TABLE - VII

System	Remarks
17. Gel-Exclusion Chromatography and optical spectroscopy demonstrates that the $(NH_3)_5$ Ru-4-(11'-dodecenyl) pyridine^{3+} ion binds to unilamellar phosphatidylcholine liposomes. Ions containing shorter ω^- alkenyl substituents showed progressively weaker binding with decreasing chain length. (Lee et al, USA)	Electron micrographs showed that the lipsomes were nearly homogeneous population of approximately spherical particles with a radii of 130 ± 15 Å and a much smaller sub population (~ a few %) with radii of 353 ± 18 Å; the sizes were unchanged on binding the Ru^{3+} complex. Addition of Chromous, Vanadous or Ascorbate ions to the vesicle suspensions gives rise to biphasic one-electron reduction of the bound Ru^{3+} complex. Slow phase step only when both inner and outer vesicle surface has Ru^{3+} complex and is proportional to area comprising the inner vesicle surface. Membrane polarization effects (e.g. addition of valinomycin or proton carrier) do not influence the reaction. No evidence for transmembrane diffusion. Liposomes containing initially only externally bound Ru(III) ions showed no slow phase upon reduction. Slow process is attributable to reduction of Ru(III) bound to the internal liposomal surface by externally added reductant. The slow step is identified with a transmembrane electron exchange between the $Ru^{2+/3+}$ ions as shown on left. Tunnelling model gives a tunnelling distance of 22 Å which is half the bilayer width. Transmembrane electron transfer may involve "hopping" conduction mechanism through the alkyl chain interface. Temperature dependence is quantitatively attributable to thinning of the bilayer membrane which accompanies lateral expansion of the vesicle with increasing temperature.

TABLE - VII

System	Remarks
18. Viologen : LEV^{2+} : N-ethyl-N'-(6-hexyl-amide)-N", N"-dihexadecyl-4,4'-bipyridinium dibromode, LEV^{2+} forms bilayer structure (vesicles or lamellae) in aqueous solutions above about 20 μM. Viologen : PSV^{2+}; N,N'-bis (3-sulfonato-propyl)-4,4'-bipyridinium, Zn meso-tetra (4-methylpyridinium) porphyrin (ZnTMPyP)-photosensitizer Triethanolamine (TEOA) : Sacrificial electron donor. Absolute quantum yields of viologen (PSV) cation radicals determined.	Highly efficient charge separation and storage of light energy in synthetic bilayer membrane of amphipathic viologen studied. At 548 nm absolute quantum yield of 0.8 was achieved by addition of as low as 25 μM LEV^{2+}. ϕ -value was found to vary with concentrations of LEV^{2+} below its CMC (20 μM). Quenching rates by LEV^{2+} was negligible as compared with PSV. Half life of transient viologen cation radicals was 90 μs in the absence of LEV^{2+} and 10.6 and 29.0 ns in the presence of 0.0025 and 1 mM LEV^{2+} respectively. The latter value is comparable with that (20.6 ms) observed in a system of ZnTMPyP and LEV^{2+} alone. These results strongly suggest that Zwitterionic viologens (PSV) shuttle, as an efficient electron mediator, between a photoreaction center (triplet state ZNTMPyP) and an electron storage pool (a bilayer membrane of LEV^{2+})
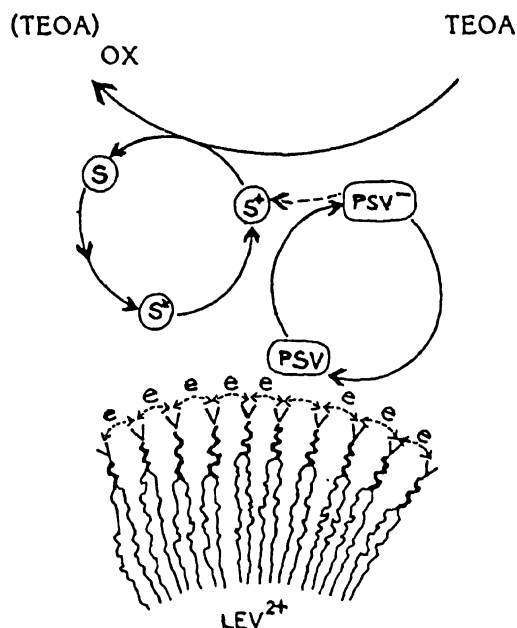
(Nagamura et al, Japan)

TABLE - VII

System	Remarks
19. Photochemical energy - converting systems using liposomes (goal) 2,6, dichloroindophenol as a mediator, sodium ascorbate as a donor and potassium ferricyanide as an acceptor - Studies showed that the rate determining step was the reaction in the aqueous phases : bulk water or inner compartment of liposomes. Thiazines with long alkyl chains immobilized in the membrane mediate transmembrane electron transport - the dye being evenly distributed on both sides of the lipid membrane.	Vectorial transport of reactants and products to retard back reactions is expected to be provided in an anisotropic medium such as liposomes. Organic redox dyes such as thiazine and indophenols mediate electron transport from an electron donor on one side to an acceptor on the other side of the membrane with the rate determining step, not being the electron transport across the membrane, but the electron transfer from the donor to the mediating dye or that from the reduced dye to an acceptor.
Two liposomal systems : Thionine mediated electron transport, in one system with ferricyanide in compartment and ascorbate in bulk water, other with ascorbate in compartment and ferricyanide in the bulk water.	Under photoradiation, electron transport via dyes in the excited state is observed and is found to be asymmetrical. It is observed that on photoreduction electron transfer is accelerated only in the system with Fe^{3+} in compartment and ascorbate in the bulk phase.
Ascorbate/Chlorophyllin/Methyl Viologen system (Nakamura and Toda, Japan)	On photoradiation 'uphill' electron transport achieved but only when methyl viologen was dissolved in bulk water.
20. Photoionization in artificial vesicles	The presence of an electric field greatly enhances charge separation in micelles, photoelectric bilayer membranes, pigmented liposomes etc.
DODAC vesicles (homogeneous) - A fluorescent dye DODCI; Rapid equilibrium paritition of DODCI between vesicles and a Dowex cation exchange studied to measure accumulation of dye with transmembrane potential (Faure et al, France)	Selective diffusion of ions through the membrane can generate transmembrane electric fields in vesicles.

TABLE - VII

System	Remarks
E. Single Crystals	
21. Dyes adsorbed on organic single crystals e.g. Rhodamine B adsorbed on Anthracene single crystal. Electron transfer studied with sub nanosecond single photon counting techniques from Anthracene to Rhodamine B on excitation of dye. Observed fluorescence has 3-exponential decay, always with a fast component of about 100 ps. (Kemnitz, Yoshimara et al, Japan)	Two advantages of such a system for studies of electron transfer : (1) geometrically fixed system and hence not affected by molecular diffusion and (2) solvent free system and hence temperature dependence can be studied to very low temperatures. Energy transfer in dyes avoided by using very low coverage of dyes on the substrate ($\sim$0.01)
F. Measurements	
22. Methods : Various kinds of electron spectroscopy such as sub nanosecond spectroscopy, Attenuated total reflection Infra-red spectroscopy, Total internal reflection Raman spectroscopy.	Time and Depth Resolved Spectroscopy - to measure photoprocess as a function of time and as a function of the distance from the interface.
System A thin film (A-film) (0.01, and 0.4 μm) coated on sapphire was doped with POPOP (p-bis2-(5-phenylene oxazolyl benzene). A thick film (B-film) (several tens of μm) contained N-ethylcarbazole as a fluorophore. Both films were contacted firmly with each other by pressing B film to the A film on the sapphire. Total internal reflectance spectroscopy carried out. (Masuhara et al, Japan)	

TABLE VIII

Summary of Posters on "Mechanism and Simulation of Photosynthesis"
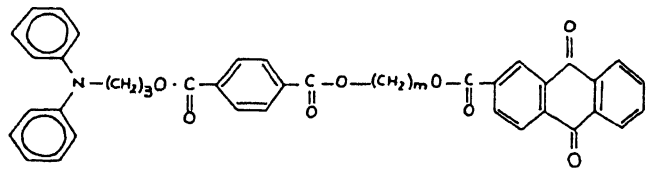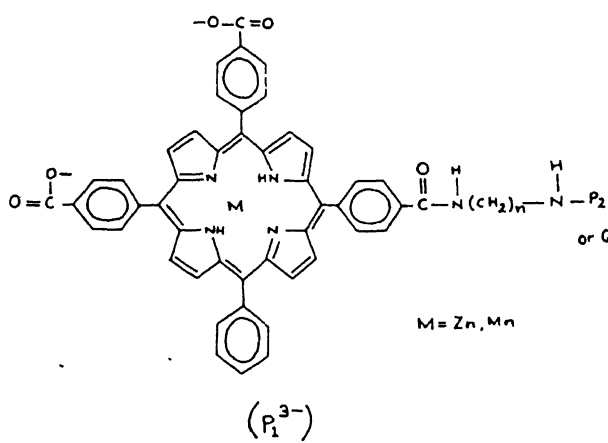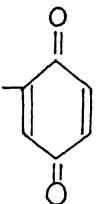
System	Remarks
1. m=3,6,8 A donor-acceptor system with a gradient of redox potential. Charge separation efficiency on photoexcitation of donor was studied in a rigid medium. (MTHF at 77 K) (Yamamoto et al, Japan)	For m = 8 the absorption band of $AQ^{\cdot}$ and $CZ^{+\cdot}$ is weak and both $CZ^{+\cdot}$ and $TP^{-\cdot}$ decay very fast. For m = 3 the absorption of $AQ^{-\cdot}$ is rather strong and the band of $CZ^{+\cdot}$ (AQ^{-}) decays very slowly. m = 6 behaves similar to m = 3. Both m = 3 and m = 6 give larger amount of AQ^{-} than m = 8. Decays of $CZ^{+\cdot}$ for m = 3 and 6 are 100 times slower than those for m = 8. Therefore when distances between CZ and TP and between TP and AQ are properly designed efficient charge separation is obtained and lifetime of pairs of ion radicals formed are prolonged.
2. Water soluble covalency linked porphyrinquinone and porphyrin dimer. M = Zn, Mn (P_1^{3-})	Interaction of these with lipid layers characterized. P_2 = Same as P_1 with the three carboxyl groups replaced by CH_3 and $-\overset{O}{\overset{\Vert}{C}}-\overset{H}{N}-(CH_2)_n-\overset{H}{N}$ replaced by $-\underset{O-}{\overset{O}{\overset{\Vert}{C}}}$; Q^{-} = $-\underset{O}{\underset{\Vert}{OC}}-CH_2-$(p-benzoquinone). In both case O^{-} of the linking carboxyl group is lost on coupling. It was reasoned that the charged tricarboxyl groups would confer water solubility upon the complexes while the hydrophobic porphyrin should insert into the lipid bilayer. Fluorescence studies in PC-vesicles exhibit much greater

TABLE - VIII
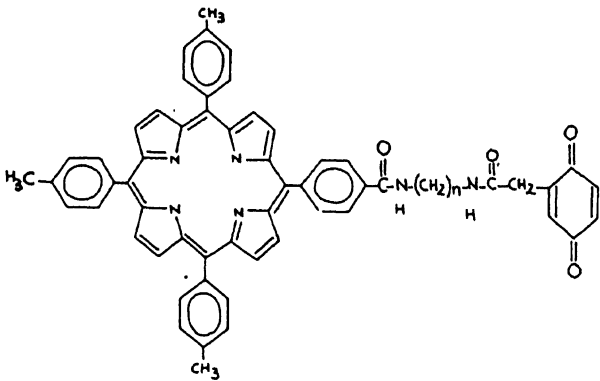
System	Remarks
(Nango et al, Japan)	efficiency of quenching with water soluble porphyrins. The results are consistent with a charge separation mechanism in which the quinone accepts an electron from the porphyrin from its singlet excited state. The Mn, P_1-Q and P_1-P_2 are being tested for catalysis of electron transfer across lipid membranes.
3. Covalently linked porphyrin quinone molecules with diamide linkage (Bolton et al, Canada and Wilford and Archer, U.K.)	Redox potentials determined in dichloromethane and other aprotic media. Porphyrin ring redox potentials are insensitive to chain length n and nature of the quinone moiety. The quinone redox potentials vary somewhat with n and with the medium. Energy of the charge separated P(+)-Q(-) state is estimated from the redox potentials to be $\sim$1.35 eV. This correlates with the photochemical observation that the charge separated state is produced from the lowest singlet state (1.91 eV), the triplet ($\sim$ 1.4 eV) being inactive.
4. PAnAR $P-\overset{O}{\overset{\parallel}{C}}-\overset{H}{N}-(CH_2)_n-\overset{H}{N}-\overset{O}{\overset{\parallel}{C}}-R$ P ⟶ substituted tetratolyl porphyrin A ⟶ amide link n ⟶ number of intervening (CH_2) groups Q ⟶ Methylbenzoquinone QH_2 ⟶ Hydroquinone DMB ⟶ Dimethoxy benzene R = Q, QH_2 DMB (Connolly et al, USA and Bolton et al, Canada)	Studied by EPR and optical spectroscopy, fluorescence spectroscopy and life times and laser flash photolysis. EPR and optical spectra reveal photo induced intramolecular electron transfer. Spin spin coupling in EPR shows that the 2 radicals are in the same molecule. $P^{+\cdot}Q^{-\cdot}$ stable for several hours at cryogenic temperature (Quantum yields of formation $\sim$ 3%). Optical differences spectrum suggest conformational change during irradiation.

TABLE - VIII

System	.Remarks
	Fluorescence and life time studies reveal existence of 2 distinct forms = a family of complexed conformers with end group folding so as to interact with the porphyrin and one or more extended conformers in which the porphyrin moiety is unperturbed by the end group. n = 3 seems to be the optimum for efficient intramolecular transfer rates ($< 1 \times 10^{8}$ to $> 7 \times 10^{9}$ s^{-}). Decay kinetics after laser flash photolysis at 110 K can be fit to three first order processes with life times of the order of 80 µs, 300 µs and 1.4 ms. The two longer-lived components are triplet states of the porphyrin with the longer-lived triplet state probably arising from extended conformers. The 80 µs species is assigned to a short-lived charge transfer state, similar to but not identical with the charge-separated radical pair state in PAnAQ. At faster time sweeps a faster kinetic component which is strongly temperature dependent is observed and this component is attributed to inter-conversions between the two conformeric families within their triplet manifolds. It is inferred that the most important geometric factor affecting the rates of electron transfer in these flexible molecules is the ability of the two moieties to assume one or more optimum configuration. Thus, stabilization of the charge-separated state may involve torsional mobility of the linking bridge which permits the quinone end group to "flip" from a complexed conformation, in which electron transfer is fast, to an extended configuration, in which reverse electron transfer is slow.
5. NH N N HN O O A meso-phenyl octamethyl porphyrin as donor; quinone acceptor and [2, 2 . 2] bicyloctane linker (Geller et al, USA)	Preparative method described and photochemistry studies just started.

TABLE - VIII
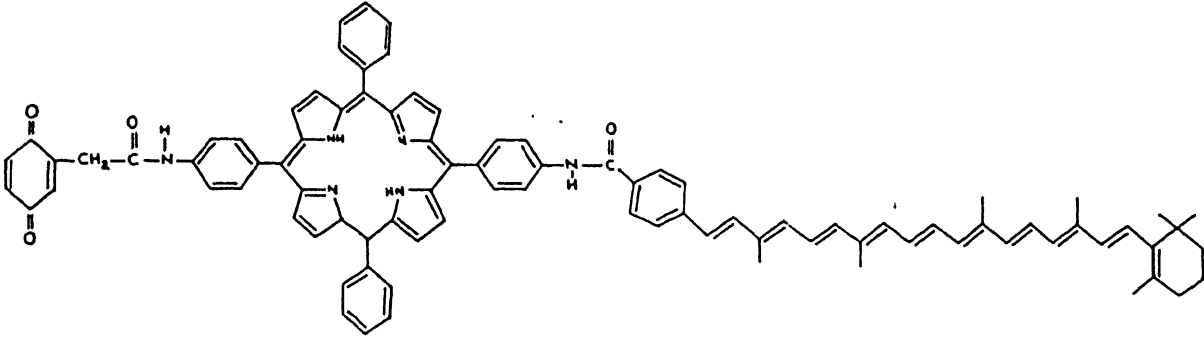
System	Remarks
6. Carotenoporphyrin - quinone triads	
(Moore et al, USA, Bensasson et al, France and Land UK)	500 MHz ^1H NMR shows that the solution conformation is an extended one with the quinone and carotenoid moieties well separated in space. Laser flash photolysis gives the carotenoid radical cation. Porphyrin $(S_1) \xrightarrow{\text{few pS}}$ charge separation to $C - P^{+\cdot} - Q^{-\cdot}$ (picosecond laser spectroscopy and fluorescence studies) $C - P^{+\cdot} - Q^{-\cdot} \xrightarrow{\text{100 pS}} C^{+} - P - Q^{-}$ (lifetime of μs in suitable solvents quantum yield $\sim$ 0.25) Redox potential of final state is $\sim$ 1V Chain length (no. of $-CH_2-$ spacers) modifies life time of the intermediate and final charge separate states. The triads mimic not only charge separation but also photosynthetic singlet energy transfer (antenna function) and triplet energy transfer (photoprotection from singlet oxygen)

TABLE - VIII
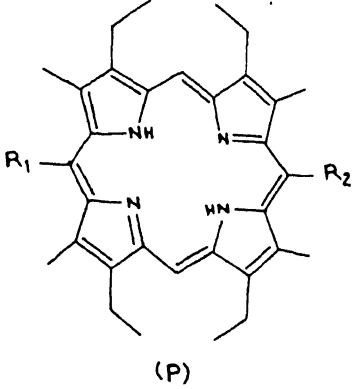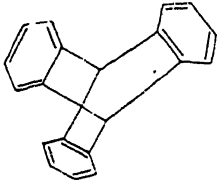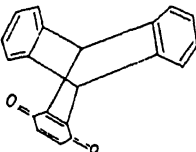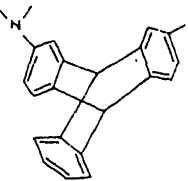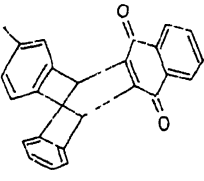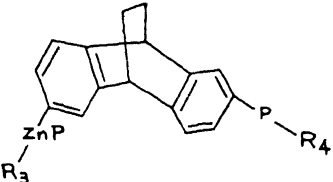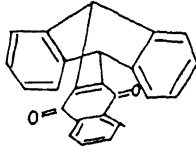
System	Remarks
7.	Synthesis of bichromophoric and trichromophoric donor-acceptor molecules with fixed donor-acceptor distance and orientation to avoid a great deal of difficulty in interpreting spectroscopic obervations with respect to detailed molecular structures when the donor-acceptor geometry is only mildly restricted. Both single step and multi-step photoinduced electron transfer chemistry have been examined. Picosecond studies show porphyrin quinone (a) forms $P^{+} Q^{-}$ in 9 ps which decays to ground state in 180 ps in butyronitrile. In presence of exogenous amine sacrificial donors stable PQ^{-} is formed. In (b) excitation leads to $P^{+}Q^{-}$ in 10 ps. Secondary electron transfer from the amine to the porphyrin proceeds in 60 ps to yield a state, most probably $D^{+}Q^{-}$ radical ion pair that lives at least 100 ns. Other such exotic comounds with fixed donor-acceptor geometry are under investigation. These are (c) and (d).

(P)

[a] R_1 R_2

[c and d]

For [c] R_3 = Phenyl
R_4 = Phenyl

For [d] R_3 = Phenyl
R_4 =

[Wasielewski et al, USA]

TABLE - VIII
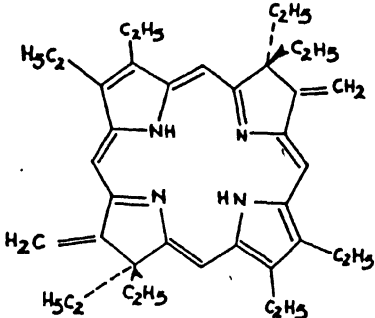
System	Remarks
8. A metal free model of BChl and bacteriopheophytin (B Pheo)b : (Fujita et al, USA)	Structure determined by X-ray diffraction. Compound is found to crystallise in two different space groups, one of which contains occluded solvent. Bonding parameters are similar in the two crystal habits. In both habits molecules pack in chains in which ring I of one molecule overlaps ring III of its neighbour with a vertical separation of 3.6A, indicative of $\pi - \pi$ inter actions. The structure mimics the structure proposed (from ENDOR) for P 870^{+}- the oxidized primary donor of bacterial Reaction Centres containing BChla. Similar overlap is exhibited by several pheophytin and chlorophyll derivaties. $\pi - \pi$ interactions, alone or enhanced by coordination of Mg in the chromophores may promote aggregation of chromophores and thereby provide a mechanism for exciton and electron migration in vitro and in vivo.
9. Electron transfer activity of the rubredoxin model complexes between FNR and Cytc examined. Rubredoxin has one Fe ion coordinated to four cysteinyl thiolato ligands e.g. Cys (6) - Thr - Val - Cys and Cys (39) - Pro - Leu - Cys (42) in C. Pasteurianum and acts as an electron mediator between flavoprotein and hemo-protein. The Fe (II) complexes of Z - Cys - X - Y - Cys - OMe (Z = benzoxycarbonyl, X - Y = Pro - Leu (1), Thr - Val (2), Ala - Ala (3)) were synthesized. The catalytic activity in electron transfer between FNR and Cyt-C was determined and found only for X-Y = (1) and not for (2) or (3). Fe_4S_4 (Z - Cys - X -	Electron transfer sequence of PSI in membrane consists of ferredoxin $NADP^{+}$ oxidoreductase (FNR), 2 Fe-2S ferredoxins and three kinds of unknown 4Fe-4S ferredoxins having relatively low redox potentials (Ca - 0.5V vs NHE). Electron transfer between FNR and some iron-protein complexes of Cys - containing peptides has been studied in an aqueous micellar solution. In native systems 4Fe-4S Ferrodoxin or Rubredoxin is known to act as an electron transfer mediator between FNR and Cyt - C. Incorporation of ferrodoxin metal complexes in micelles or vesicles seems significant as a first step for the experimental stimulation system with a forward electron transfer sequence. Iron

TABLE - VIII

System	Remarks
Y - $(OMe)^{2-}$ with X - Y = Gly - Ala (4), Pro - Val (5) and Fe_4S_4 (Z - Cys - Gly - Ala - Cys - $OMe)^{2-}$ (6) were synthesized as a ferredoxin model complex which has NH --- S hydrogen bonding and/or chelating Cys - X - Y - Cys units. Efficiency of electron transfer in presence of these 4Fe-4S complexes (4, 5 and 6) examined since redox potential of (6) (- 0.70 V for $2^-/3^-$ vs SCE) is close to those of native ferrodoxins. These model complexes have also an irreversible $2^-/1^-$ redox cycle which is close to the redox potential of Cyt-C. In contrast native ferrodoxin employs only a stable redox couple of $3^-/2^-$ for the electron transfer between FNR and Cyt-C (Ueyama et al, Japan)	protein model complexes (1) and (6) with suitable redox potentials for electron transfer in the biological system are stable in an aqueous micellar system. However, the 4 Fe-4S Ferredoxin model complexes have a $2^-/1^-$ redox couple while a $3^-/2^-$ redox couple is to be utilized.
10. Tetra 2, 3, - Pyridinoporphyrazines (1) (2) is same as 1 with a, b, c and d replaced by CH_3-pyridinium (N^+) and is water soluble.	These differ from phthalocyanines by the annelated electron-withdrawing pyridino ring. Also (2) does not aggregate in aqueous solution which could deter photochemical redox reactions.
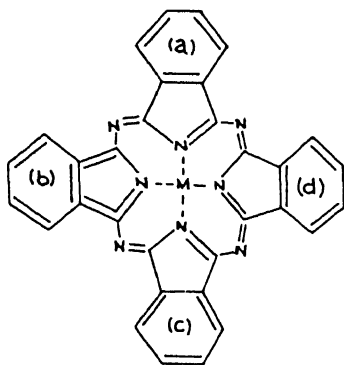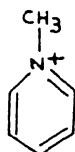
TABLE - VIII
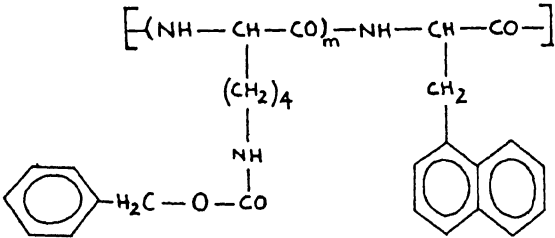
System	Remarks
1 + EDTA + MV^{2+} $\xrightarrow[DMF/H_2O\ solu.]{visible\ light}$ $MV^{+\cdot}$ Velocities (M = Al(OH) > Cd > Mg > Zn > 2H) Also a photoredox reaction occurred in the absence of methyl viologen. With (2) (M = Zn) stronger tendency toward reactive quenching in presence of EDTA is found. Chelates 2 are effective in a double sensitization using EDTA as a donor (Gitzel, et al, FRG)	Laser flash photolysis gives life time of 5.10^{-4} sec. for excited 2 (M = Zn) and life times are not influenced by methyl viologen but donors. Both 1 and 2 are highly effective sensitizers for reactions taking place via reductive quenching.
11. A sequential polypeptide carrying naphthyl chromophores $[(NH—CH—CO)_m—NH—CH—CO—]$ $(CH_2)_4$ CH_2 NH $H_2C—O—CO$ (Sisdo et al, Japan)	One-dimensional aromatic crystals as an efficient antenna system. Geometry of polypeptide inferred from circular dichroism and conformational energy calculations. CD indicates a helical arrangement of the naphthyl groups along the polypeptide chain. Fluorescence spectrum did not show any evidence of excimer formation, indicating the absence of contact between chromophores. Molecular models based on conformational energy calculations suggest that the chromophores are organized in a manner that the interchromophore distance is not so close to form contacts, but short enough to achieve an effective energy transfer.
12. Xanthene dyes as antenna molecules. A mixture of Fluorescein, Eosin Y and Rose Bengal act as the "antenna molecules". These dyes transfer triplet energy to the reaction centre containing anthracene-9-carboxylate anion (aa^-) MV^{2+}, EDTA and colloidal Pt. (Sasse et al, Australia)	Three xanthene dyes that absorb light at different wavelengths and transfer triplet energy to an acceptor molecule which then initiates electron transfer reactions that lead to the production of hydrogen. These dyes, either singly or combined act as sensitizers but the output of hydrogen is reduced, in the absence of aa^-. In the presence of (polyvinyl/pyrollidone)

TABLE - VIII

System	Remarks
	and with the reaction centre, the production of hydrogen is greatly improved.
13. Two photosystem communicating through a Nafion membrane previously doped in $Ru(bpy)_3^{2+}$ and covered with a RuO_2 layer : PSI = $Ru(bpy)_3^{2+}$ + MV_2^{2+} + colloidal Pt, PS II = $Ru(bpz)_3^{2+}$ + RuO_2 in a two compartment cell with optical windows; pH differential to establish a proton flow parallel to the electron flow. Two halogen lamps of 275 W were used. (Velasco, Spain)	Higher rates of gas production with the start of illumination. After two hours the process stops. No correlation between the amount of H_2 and O_2 produced.
14. Photoelectrochemical cell using chloroplast-methyl viologen systems	
a) Water photolysis using isolated spinach chloroplast-methyl viologen; sandwich type cell. anode = SnO_2, optically transparent; cathode = Pt; anolyte = Chloroplasts, methyl viologen, glucose, glucose oxidase, ethanol, NH_4Cl; buffer (pH 7.8); catholyte = 0.5 MH_2SO_4 degassed with nitrogen.	a) Hydrogen evolution without external bias observed.
b) Immobilized chloroplasts in 2 wt % agar gel attached to the SnO_2 electrode (optimum thickness 0.8 mm)	b) Photocurrent about 3 to 10 times larger than in (a). Solar energy efficiency (1 to 2%). Immobilized chloroplasts could be stored longer and retained more than 50% of their activity on storage for 10 days at 4°C in the dark.
c) Photosystem I particles extracted from phytolacca americanna with ascorbate and DPIP as the electron donor system. (Iida et al, Japan)	c) Activity persisted for about 150 hrs. producing hydrogen at a rate of 1-2 μ mol/mg chl/hr. After 24 hrs. 64% of the initial anodic photocurrent observed.

TABLE - VIII

System	Remarks
15. Hydrogen producing bacteria (Citrobactor freundii) were immobilized in Ca-alginate beads (2, 3 mm diameter). Similarly photosynthetic bacteria (R. Rubrum) which produced hydrogen from the organic acids (acetic acid, lactic acid etc) produced by C. freundii were also immobilized. Two separate bioreactors were used the one with R. Rubrum being illuminated (5000 lux.) (pH 6.8 - 7.0; 30°C) (Karube et al, Japan)	Molasses was continuously transferred to the reactors. Hydrogen was continuously evolved for 150 hours and was transferred to the anode of a phosphoric acid fuel cell, oxygen was also transferred to the cathode. Only 50% of the chemical oxygen demand of the molasses was removed in the 2 bioreactors, Optimization is required.
16. Biophotolysis of water	Research focussed in three areas of biophotolysis of water :
1) For wild type chlamydomonas efficiency of 2 to 3% in the low intensity linear portion of the light saturation curve obtained.	1) Absolute thermodynamic conversion efficiencies of intact microalgal entrapped as thin films.
2) Current experiments on intact thylakoid membrane as well as fractionated and differently centrifuged components support the concept of a partitioning of the photosynthetic photoreactions according to the morphological structure of the thylakoids.	2) Stoichiometric ratio and location of the photoreaction of photosynthesis.
3) Functional stability was short lived when immobilized in carrageenan, alginate and agar gels. It appears that although chloroplasts immobilized in gels and chemically cross-linked glutaraldehyde have improved storage stability over free chloroplasts, they are at present not suitable for the long term biophotolysis of water.	3) Reconstitution and immobilization of extracted chloroplasts, ferredoxin and hydrogenase.

TABLE - VIII

System	Remarks
4) Algal H_2 and O_2 photoproduction After 3 generations of selection, yields of H_2 from photosynthesis were improved by approximately 37% (chlamydomonas reinhardtii) (Greenbaum et al, USA)	4) Long term endurance and photosynthetic mutant studies.

A molecular energy storage system is composed of an endergonic reaction leading to a high energy compound which is stable but will undergo the reverse exergonic process with a catalyst and release energy in the form of heat.

$$A \xrightarrow{h\nu} B$$

$$B \xrightarrow{\text{catalyst}} A + \text{heat}$$
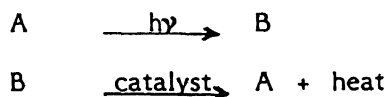
Yoshida (Japan) in his plenary talk identified several conditions that such a system should fulfil for being viable. These are : 1) Reactant A must absorb UV and visible region of sunlight. The absorption band of A should be toward visible region and have low intensity ($\epsilon \simeq$ 10 to 100). It may be possible to use a photosensitizer but side reactions due to photosensitizer makes it dirty. Introduction of chromophore increases molecular weight and therefore energy storage value decreases; it also leads to photodegradation of chromophore with sunlight. In norbornadiene, introduction of chromophore decreases quantum yield. 2) Reactant A should be photochromic, and photo product (valence isomer B) must not absorb sunlight. This is partly achieved by skeletal reorganizations e.g. π bond $\longrightarrow \sigma$ bond. 3) The quantum yield for reaction A $\longrightarrow$ B must be near unity even in the presence of oxygen (usual quantum yields for a photo-organic reaction is 10^{-3} to 10^{-2}). 4) Reaction A + B must have a large positive ground state enthalpy (high energy storage value, ES). The ES must be larger that 100 kJ/kg. 5) The photoproduct B must be stable and bear the long term storage at ambient temperatures. 6) Reaction B $\longrightarrow$ A must be controlled by a catalyst. 7) In the presence of air (oxygen) Reactions A $\longrightarrow$ B and B $\longrightarrow$ A must proceed quantitatively. Even though it seems quite impossible to satisfy all these conditions and most have declared this mode of solar energy conversion and storage as unviable, Yoshida presented new molecular energy storage systems (A/B pair) which satisfy reasonably the conditions stated. The new system synthetically engineered consists of a non-conjugatively bound pair of donor olefin and acceptor olefin. Such a system with norbornadiene had new absorption bands. The quadricyclene formed from such a substituted norbornadiene had a life time of years compared to days for the unsubstituted quadricyclene. New catalysts for B $\longrightarrow$ A transformation are found to be in Pd-cyclopropane complex, Ag etc. It is better if the catalyst is immobilized such as specific Co (II) complexes in alumina (cobalt-heme catalyst). A system called DONAC has
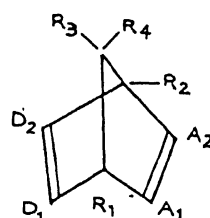
is synthesized easily:

$+ A_1\text{-}C{\equiv}C{\equiv}A_2 \longrightarrow$
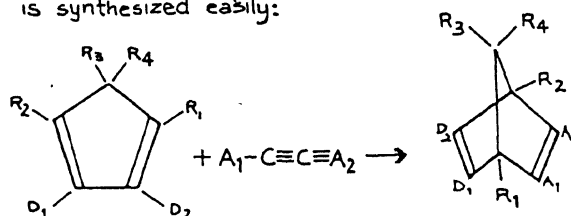
The new DONAC systems have the following features : (1) A/B system can be clearly recycled for long periods; (2) Transformation from A to B is easily observed by colour change (A is colored and B is colorless); (3) Temperature of A does not rise when solar energy is stored. (4) Compound B in solid form stores energy for infinite periods at ambient temperature, in the absence of a catalyst. (5) 1 kg of B could release 120 - 130 Kcal energy. (6) A and B are stable to oxygen and humidity. A bench pilot model using Fresnel lenses and optical fibres has been constructed and is under test (La Foret Engineering Co., Himamori). It is interesting to note that Yoshida has made spectacular advances by elegant organic synthesis in an area which has been given up in most countries. In fact among the ten posters presented in this area (Table IX) nine were from Japanese laboratories.

TABLE IX

Unimolecular Storage - Summary of Posters
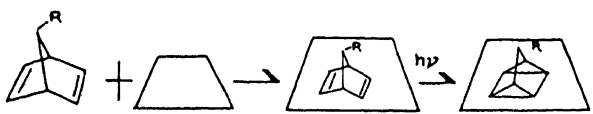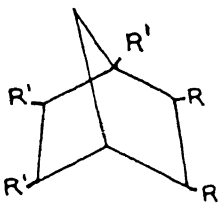
System	Remarks
1. 7-substituted Norbornadiene-Cyclodextrin inclusion complex R = H, CH, $OCOCH_3$, $OC(CH_3)_3$ (Yumoto et al, Japan)	-OH, acyloxy, alkyloxy groups substituted in 7-position removes the offensive odour of Norbornadiene (NBD) and functions well as organic heat storing agents. The inclusion complexes have no smell of original NBD's. Studies showed that the 7-substituted inclusion complexes can be converted into its isomer with no side reaction in the solid state as well as in the liquid state. Acetophenone as sensitizer improved the rates of photoisomerization.
2. R = CN, R' = CH_3 Sensitization by $Ru(bipy)_3^{2+}$ with 546 nm (Kutal, USA and Ikezawa et al, Japan)	10^{-3}M solution of the substituted NBD absorbs out to 420 nm. Direct photolysis yields the quadricyclene isomer (QC) with quantum yields of 0.68. Sensitization is believed to occur by quenching of the emissive metal to ligand charge transfer excited state of $Ru(bipy)_3^{2+}$.
3. a) Stabilization of the norbornadiene system by antioxidant such as Ionol and sensitizatin by acetophenone found to cause polymerization of the NBD. Usage of Ionol with m-methoxy acetophyenone as the sensitizer excludes the polymerization.	Hybrid solar water heating plant designed and efficiencies between 0.4 to 0.6% for three different types of collectors.

TABLE - IX
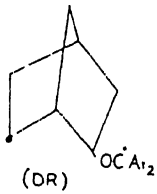
System	Remarks
b) Catalyst for back isomerization of QC ⟶ Poly - Cobalt phthalocyanine (Co-PPC) adsorbed and supported on active charcoal beads or cobalt tetra-phenyl porphyrin (CO-TPP) supported on polystyrene. Co-PPC yielded better turnover number and has a long life. (Ohaku et al, Japan)	
4. Sensitization of NBD ⟶ QC conversion by a series of benzophenones - Quenching rate constants determined by laser spectroscopy. It is suggested that the sensitization proceeds through addition of the n,π^* triplet state of the sensitizer to the unsaturated bonds of NBD to give adduct diradicals (DR) which subsequently undergo intramolecular cyclo addition or elimination of the sensitizer molecule. $^3Ar_2CO^* + NBD \longrightarrow$ (DR) [structure with $\dot{O}CAr_2$]; $DR \longrightarrow QC + Ar_2CO$ (Sakuragi et al, Japan)	The sensitizing action is not a simple energy transfer but the efficiency of the reaction is strongly influenced by the nature of the substituents rather than by the triplet excitation energy of the sensitizers. The more electron-donating substituents in the sensitizer, the more effective is sensitization if the triplet excitation energies are nearly the same.
5. Water soluble NBD derivatives to avoid use of organic solvents. A is highly soluble in alkaline solution and is stable in a boiling sodium carbonate solution. Also absorption wavelength is shifted towards longer λ	The photo isomerization to corresponding QC was quantitative with quantum yield of 0.08 ± 0.01 at 313 nm in presence of air. Cobalt tetra (p-sulfophenyl) porphyrin catalyses the back reaction with release of heat very efficiently. However water insoluble catalysts are preferred

TABLE - IX
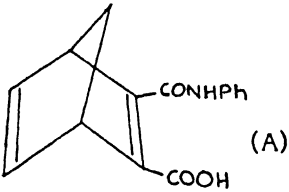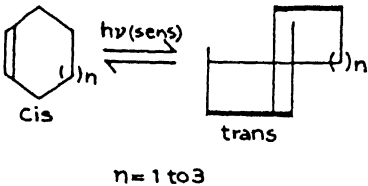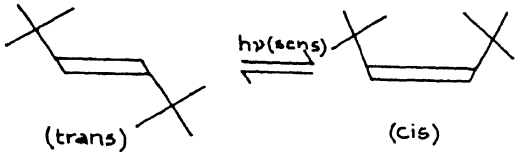
System	Remarks
 Maruyama et al, Japan)	and these are found to be cobalt tetraphenyl porphyrin or cobalt phthalocyanine on activated carbon. These catalysts are very efficient. Strained alkenes produced photochemically could store solar energy. The yields of more strained forms are better in direct than in sensitized excitation.
5. (Inoue et al, Japan)	Strained alkenes produced photochemically could store solar energy. The yields of more strained forms are better in direct than in sensitized excitation.
7. Diels alder adducts of phosphole derivatives examined for their photo-chemical reactivity. (Tomioka and Izawa, Japan)	With acetophone P-containing caged products are obtained.
8. Photodimerization between two cinnamic acids to form cyclobutane ring is controlled by the topology when trans-cinnamoyl moieties are bound at ends of a polyethylene glycol chain. The podants may also trap cations. The topo-	The effect of the chain length and cation effect studied.

TABLE - IX

System	Remarks
logy is controlled by the length of the chain and the formation of cation complexes. (Kimura et al, Japan)	
9. Hydroazulenes (Knoechel et al, FRG)	Photochromism observed and studied; attributed to valence isomerization.
10. Meta-substituted polycarbonyl compounds (triplet lift times (τ_T)) of substituted 1) 2, 4, 6-triisopropylbenzophenones (3' or 4' - X) and 2) substituted 2, 4, 6-triethylbenzophenones (3' or 4' - X) studied with X = 4' - OMe, 4' - Me, 3' - Me, 4' - Cl, 3' - CoPh 4' - CF_3 R = isopropyl in 1 series = ethyl in 2 series (Matsuara and Ito, Japan)	Steric control in localization of electronic excitation energy. The correlation of τ_T in a Hammett plot is found to be opposite between series (1) and series (2). It is believed that in series (1) there is slow rotation around 1 - α and 1' - α ; in series (2) there is free rotation around these bonds and the triplet life times are controlled by the rate of intramolecular abstraction from the benzylic position.
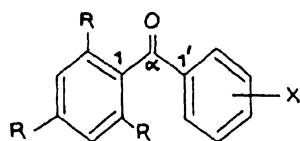
CONCLUSION

At the concluding session chaired by Sir George Porter, it was emphatically stated that while very good progress has been made in the area of photochemical conversion of solar energy, one has not achieved any viable storage possibility which is the crucial advantage of the chemical route. One realises that the competition from solid state photovoltaic cells, especially amorphous silicon is very steep. Thermal systems also have to be contended with. Here again storage is the crucial factor that can justify the chemical route.

In the area of homogeneous and heterogeneous catalysts considerable progress has been made in identifying sensitizers and relays but the conversion of the absorbed energy into a stored form in fuels is still inefficient. So one is forced to identify new systems including new catalysts and study their fundamental properties before an attempt is made to produce fuels. In particular, the area of photocatalysis by particulates seems to be emerging as a new synthetic route. It is believed that it is better to focus on those chemical reactions which cannot be carried out by a combination of a photovoltaic system and an electrolysis system. The role of hybrid catalysts Cd(S, Se); ZnCdS (solid solution) and the role of functionalized surfaces for achieving high selectivity and reactivity and some times even stereospecificity in chemical synthesis is found to attract great attention. There was a plea for generating a standard for photocatalyst (e.g. TiO_2/Pt or CdS/Pt) with prescribed methods of preparation, crystallinity, surface, particle size, pre-treatment and methods of Pt deposition.

Organized molecular assemblies would become more and more fanciful with the innovativeness of the synthetic chemist being the deciding factor, Monolayers, micelles, polyelectrolytes, bilayer membranes and colloids would attract attention and it is feasible that from ten years now we may have devices engineered on principles of molecular electronics. Many basic principles have yet to be understood regarding electron transport mechanisms in such systems.

Heller (Bell Lab, USA) was most emphatic in claiming that the investment of $ 200 million in research and development efforts towards photoelectrochemical cells has already paid off (way beyond what has been invested). He identified the following to have benefitted by such research efforts; photoconversion to manufacture IV - V compounds; photodeposition of metals; photooxidation of organic compounds leading to new paints (non-flaking, non-choking paints); phototransport of metals beyond diffraction limit and gas sensors. He further identified the following as products already developed or near commercial development : Polymer coated semiconductor electrodes as biosensors; semiconductor complexes with metals as ultrafast photodiodes; new photographic dyes; development of selective photooxidation of pollutants with semiconductors; photooxidation of films. In essence, this effort has created a new photon-based industry. The chance of production of electricity does not seem to be remote now as it did a few years ago. Liquid function cells have achieved higher efficiencies than amorphous Si PV cells, with comparable stability as amorphorous Si devices but poorer reliability. It is imperative to address research to packaging, transport etc. The conference concluded with an encouraging note that research and development in the area of photochemical conversion and storage of solar energy would definitely contribute to the economic growth of the world.

The developed countries such as USA, Japan and European countries have signed an agreement, at this conference, to pool their resources and research effort to achieve a major break through in this important area of scientific and technological endeavour.